BONE MINERAL DENSITY MEASUREMENT USING DEEP NEURAL NETWORK WITH SMART TRACKING SYSTEM

CHAPTER 1

ABSTRACT

Image processing is a widely used domain and it's applied in various fields. Biomedical imaging is one of the research areas of image processing which is used to detect diseases. Biomedical imaging consists of various subresearch areas such as bone imaging, arthritis imaging, bone imaging and blood cells imaging. The proposed work comes under bone imaging and the objective is to detect the occurrence of Arthritis. Bone mineral density (BMD) measurements are the gold standard by which osteoporosis is diagnosed. Dual Energy X-ray Absorptiometry (DEXA) is the most commonly used measuring technique to assess BMD at both the hip and spine. There are three sites within each hip, collectively called the femoral sites, which are assessed—the femoral neck site, the trochanteric site, and Ward's triangle. It is a known fact that the different areas of the femur are composed of different percentages of cancellous bone. Arthritis is an autoimmune disease that mainly affects the joints in the human body. Bone organ plays a vital role in identifying these types of diseases. Manual analysis of bone images is a long term process which needs an expert orthopedist for continuous assessment of bone scans which is costly and time consuming. The proposed work involves steps such as image restoration, image enhancement and smoothing, bone segmentation and edge detection in order to enhance the given image and separate the region of interest. The strength of a bone depends on Bone Mineral Density (BMD) which is a major factor in identifying bone diseases and fracture risk. The mathematical relationship between Bone Mineral Content and Volume by Region of Interest will helps in calculating Bone Mineral Density and various features of bone images such as area, mean, standard deviation and variance. The Gray Level Co-

occurrence Matrix (GLCM) is one of the image analysis techniques that can be used for extracting features (Energy, Entropy, Contrast, Homogeneity and Correlation) of a bone image. A dataset is created from both the normal and eroded bone images by applying BMD and GLCM features. The deep neural network is used to classify whether the given image is normal or abnormal. The MATLAB serial communication port is enabled to communicate with the hardware device which is connected with the GSM module to communicate with the doctor and other responsible persons regarding the patient's abnormality condition. The hardware design of this patient monitoring system is based on 8051 microcontroller. Microcontroller acts as the gateway to GSM module. Wireless communication module has the advantage of lower power consumption which is attractive for portable applications. This system provides safe and accurate monitoring. It also gives the freedom of movement. The proposed system can be used to monitor the physiological condition of a person.

INTRODUCTION

Visual representation of body parts, organs and tissue is used in diagnosing diseases. In order to create images of body parts for clinical aspects medical imaging is used. Medical imaging provides services for radiologists, radiographers, medical physicists and biomedical engineers to diagnose disease accurately. Medical imaging consists of many advantages: Images are creating an atmosphere for the doctors to diagnose diseases as much as earlier possible. Medical imaging improves the quality of patient results, decrease hospitalization and replace invasive surgeries. Medical imaging produces enormous amount of data and quality of patient care depends on how fast and effectively this data can be turned into high resolution diagnostic images. In real world many people think that Arthritis is a single disease but Arthritis refers to group of more than 100 diseases

related to joint stiffness, joint pain and joint inflammation. It not only affects people who are aged but also of all ages, races and genders. Abnormal behavior of cells is a major reason to Arthritis and it's called as chronic that mean long term disease. Some drugs are also used to treat Arthritis. In this work, we made an attempt to create an automated tool to diagnose Arthritis as accurate as possible. Basically our immune system should protect our body from foreign cells like bacteria and viruses. Arthritis is an autoimmune disease which mainly attacks tissue and joints present in the body. Abnormal behavior of immune system causes inflammation that can damage joints and organs. Early morning pain, stiffness, swelling, fatigue and warm, swollen, reddish joints are the symptoms of Arthritis. Early diagnosis and advanced treatment can control the progress of Arthritis even though there is no known cure for Arthritis.

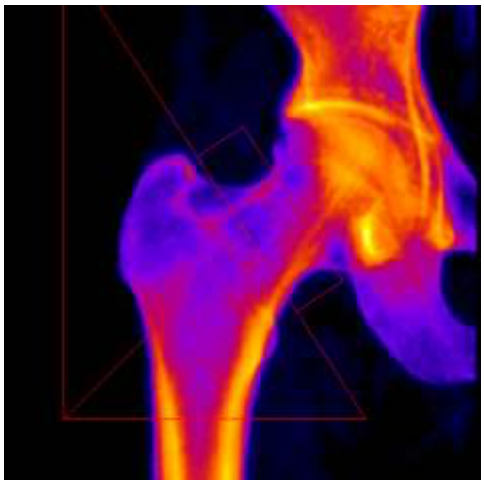

OBJECTIVE

To design a prototype for bone decease affected patient with social relevant concept to protect the patients from unpredictable accidents during walking, playing or working at the work place. If the bone density abruptly changes, the system should communicate to the appropriate persons or doctors about the patient's condition.

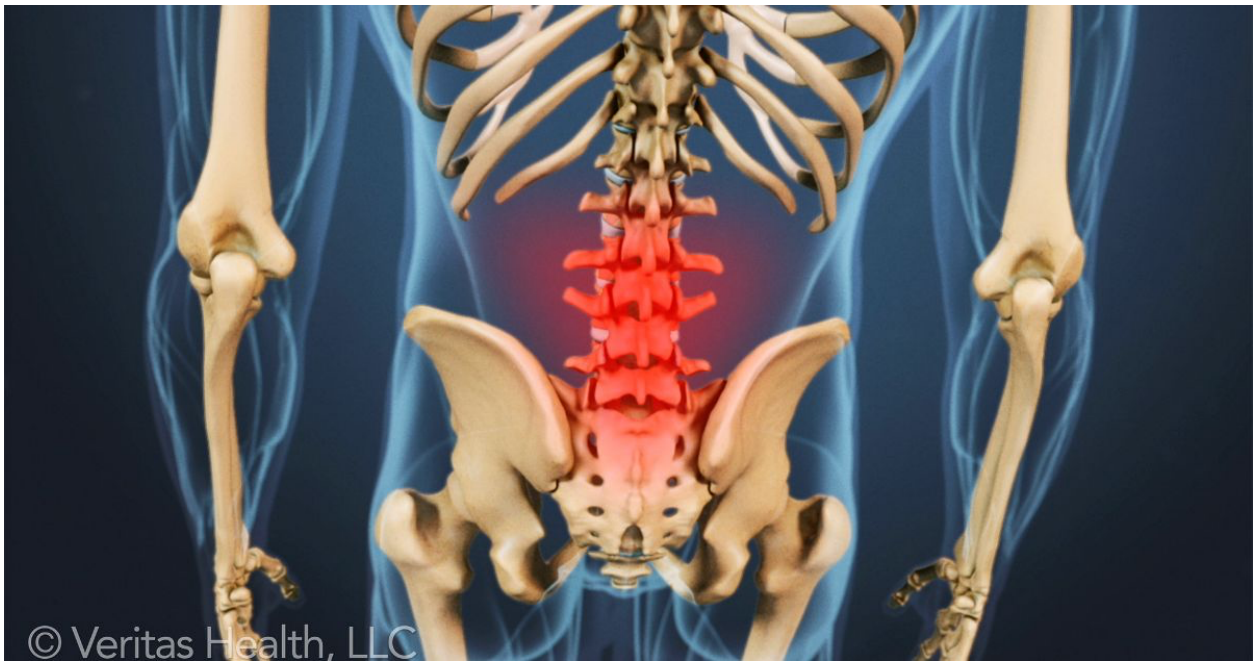

EXISTING SYSTEM

Saliency region based Region-growing segmentation for bone segmentation

The existing system segment the bone image using Saliency region based Region-growing segmentation algorithm.

DISADVANTAGES OF EXISTING ALGORITHM

- The region growing segmentation is not preferred for its limited range of applications and automatic features are not having accurate values.

- Pre-processing experiments are needed to find which type of filtering will be more beneficial. This increases the effect of the speckle noise and Gaussian noise bone images.

- The desired bond density area is selected from the segmented image to calculate the volume. The volume of the desired bone density affected area is greater than the original area. The region growing algorithm will segment not only the affected area but also the non affected area which has high intensity ratio.
- This algorithm fully depends on the intensity of the image not the shape and texture. So the accuracy and sensitivity is low.

PROPOSED ALGORITHM

DIGITAL IMAGE PROCESSING

Algorithm 1 - (Image Pre-processing Step 1 – Image Denoising (Restoration))
Algorithm 2 - Image Enhancement using Contrast Limited Adaptive Histogram Equalization (CLAHE algorithm)

Algorithm 3 – Bone Mineral segmentation using Modified Fuzzy C Means Clustering Segmentation

Algorithm 4 – Bone Mineral Density Measurement using Feature Extraction using Principle Component Analysis (PCA) and Gray Level Co-occurrence Matrix (GLCM)

Algorithm 5 – Classification using Deep Neural Network (DNN) (Normal or Abnormal)

Embedded Systems
Algorithm 6
Patient Tracking

IMAGE PREPROCESSING

Algorithm 1

Image Restoration

Proposed Algorithm 1
(Image Pre-processing Step 1 – Image Denoising (Restoration))

Image De-noising using Anisotropic Diffusion fusion Filter

The simplest and best investigated diffusion method for smoothing images is to apply a linear diffusion process. We shall focus on the relation between linear diffusion filtering and the convolution with a Gaussian, analyze its smoothing properties for the image as well as its derivatives, and review the fundamental properties of the Gaussian scale-space induced by linear diffusion filtering.

Proposed Algorithm 2

(Image Enhancement)

Image Enhancement using Contrast Limited Adaptive Histogram Equalization (CLAHE algorithm)

Adaptive histogram equalization (AHE) is a computer image processing technique used to improve contrast in images. It differs from ordinary histogram equalization in the respect that the adaptive method computes several histograms, each corresponding to a distinct section of the image, and uses them to redistribute the lightness values of the image. It is therefore suitable for improving the local contrast of an image and bringing out more detail.

However, AHE has a tendency to over-amplify noise in relatively homogeneous regions of an image. A variant of adaptive histogram equalization called **contrast limited adaptive histogram equalization** (CLAHE) prevents this by limiting the amplification.

Proposed Algorithm 3

(Image Segmentation)

Modified Fuzzy C Means Clustering Segmentation

The bone mineral density segmentation of imaging data involves partitioning the image space into different cluster regions with similar intensity image values. The bone mineral density images always present overlapping gray-scale intensities for

different tissues. Therefore, Modified fuzzy clustering methods are particularly suitable for the segmentation of bone mineral density images. There are several Modified FCM clustering applications in the THERMAL segmentation of the bone. The Modified Fuzzy c-means (FCM) can be seen as the fuzzified version of the k-means algorithm. It is a method of clustering which allows one piece of data to belong to two or more clusters. This method is frequently used in pattern recognition. The algorithm is an iterative clustering method that produces an optimal c partition by minimizing the weighted within group sum of squared error objective function.

Proposed Algorithm 4

Bone Mineral Density Measurement using Feature Extraction using Principle Component Analysis (PCA) and Gray Level Co-occurrence Matrix (GLCM)

Features are said to be properties that describes the whole image. It can also refer as an important piece of information which is relevant for solving the computational task related to specific application. The purpose of feature extraction is to reduce the original dataset by measuring certain features. The extracted features acts as input to classifier by considering the description of relevant properties of image into feature space

The Following GLCM features were extracted in our research work: Autocorrelation, Contrast, Correlation, Cluster Prominence, Cluster Shade, Dissimilarity Energy, Entropy, Homogeneity, Maximum probability , Sum of squares, Sum average, Sum variance, Sum entropy, Difference variance,

Difference entropy, Information measure of correlation, information measure of correlation, Inverse difference normalized.

Proposed Algorithm 5

Algorithm 5 – Classification using Deep Neural Network (DNN) (Normal or Abnormal)

We propose Deep convolutional Neural Network to classify whether the given image is normal or abnormal.

Proposed Algorithm 6

Smart tracking information for patient through GSM module

GSM module is used to establish communication between a computer and a GSM system. GSM module consists of a GSM modem assembled together with power supply circuit and communication interfaces (like RS- 232, USB, etc) for computer. GSM MODEM is a class of wireless MODEM devices that are designed for communication of a computer with the GSM network. It requires a SIM (Subscriber Identity Module) card just like mobile phones to activate communication with the network. Also they have IMEI (International Mobile Equipment Identity) number similar to mobile phones for their identification. A GSM MODEM can perform the following operations:

1. Receive, send or delete SMS messages in a SIM.
2. Read, add, search phonebook entries of the SIM.
3. Make, Receive, or reject a voice call.

ADVANTAGES OF PROPOSED SYSTEM

- It is good for convergence of gradients of the image pixels.
- It is the fastest algorithm when compared to the k means algorithm and Fuzzy C Means algorithm.
- The proposed algorithm can have linear convergence and the speed is based on how many information is lost.
- The algorithm is applicable for RGB colour space images.
- The best similarity difference between the pixel intensity and region mean value is properly given by the proposed algorithm. So the exact region of interest can be segmented.
- The automatic seed select is possible for image segmentation. So the accuracy of the segmentation is high.
- The automatic feature extraction using Gray level co-occurrence Matrix is possible which features are used for SVM classification.
- The algorithm depend not only the intensity but also depend on the shape and texture. So the segmentation of the object and pixel is proper.
- The proposed algorithm is applicable for both gray and RGB color space images.

BLOCK DIAGRAMS

BLOCK DIAGRAM FOR DIGITAL IMAGE PROCESSING

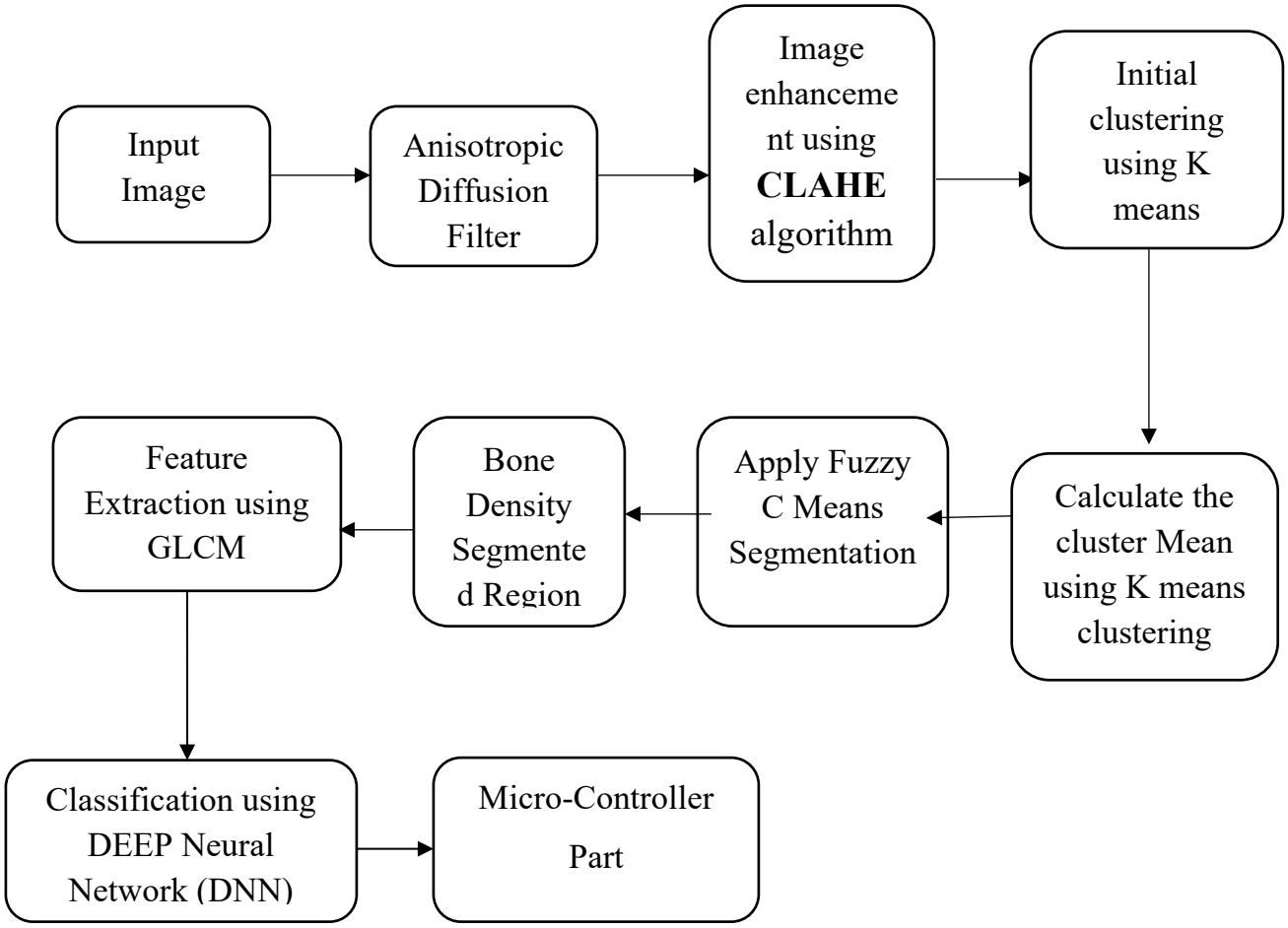

BLOCK DIAGRAM FOR MICROCONTROLLER

Smart tracking information for patient through GSM module

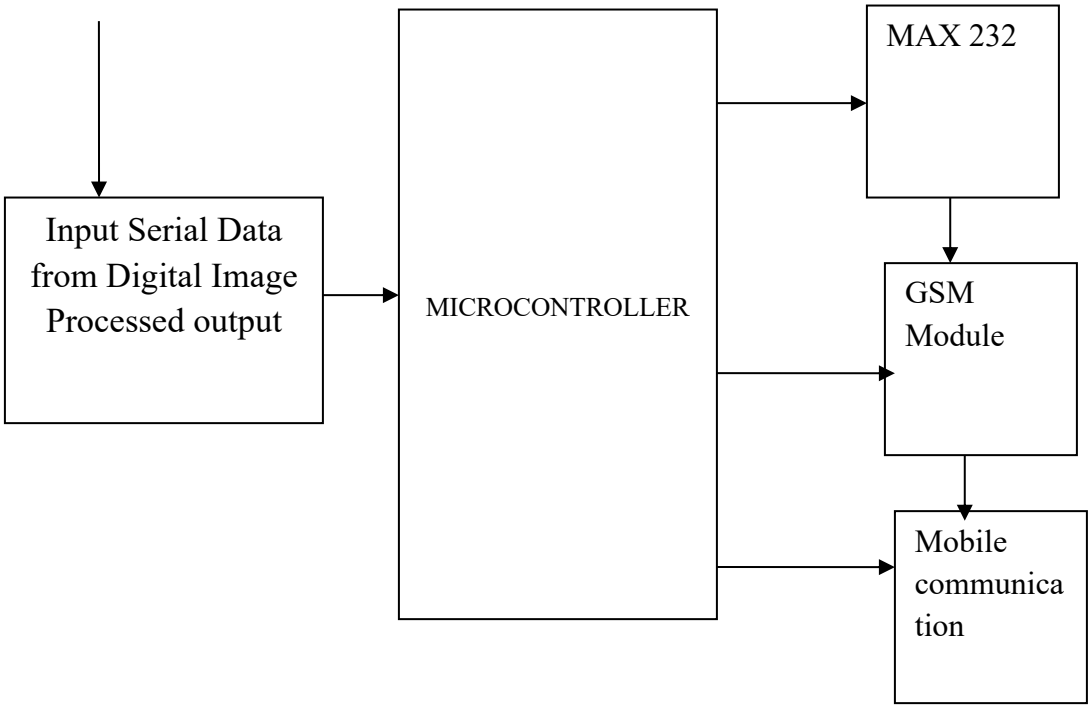

LITERATURE SURVEY

J Bone Miner Res. 1997 Jan;12(1):124-35.

Sources of variability in bone mineral density measurements: implications for study design and analysis of bone loss.

Nguyen TV[1], Sambrook PN, Eisman JA.

Measurement of bone mineral density (BMD) is a useful tool for monitoring efficacy in osteoporosis therapy. However, the ability to detect true change for a subject as well as for a group of subjects is dependent on the precision of the measurement. In this work, short-term and long-term reliability of bone mass measurements were examined at the spine and femoral neck using dual-photon and dual-energy X-ray absorptiometry and related to guidelines for study design. The concepts involved in these analyses are relevant to a study for any therapy involving a quantitative trait. Short-term reliability was assessed by repeated measures in 60 subjects aged 46 +/- 9 years (mean +/- standard deviation [SD]), and in 32 elderly subjects (aged 75 +/- 5 years), on the same day with repositioning. Long-term variability in the rate of linear changes in BMD was assessed in a cohort of 293 women and 184 men, aged 60+, each having BMD measured on three separate occasions over an average interval of 2 years. Short-term variability in BMD was assessed using the coefficient of reliability (R) and standard deviation (SD) of measurement error. Long-term variability in BMD was modeled by linear regression.

Bone mineral density: testing for osteoporosis

Angela Sheu, Advanced trainee[1] and Conjoint associate lecturer[2] and Terry Diamond, Senior endocrinologist[1] and Associate professor, Endocrinology[2]

Primary osteoporosis is related to bone loss from ageing. Secondary osteoporosis results from specific conditions that may be reversible.

A thoracolumbar X-ray is useful in identifying vertebral fractures, and dual energy X-ray absorptiometry is the preferred method of calculating bone mineral density. The density of the total hip is the best predictor for a hip fracture, while the lumbar spine is the best site for monitoring the effect of treatment.

The T-score is a comparison of the patient's bone density with healthy, young individuals of the same sex. A negative T-score of –2.5 or less at the femoral neck defines osteoporosis.

The Z-score is a comparison with the bone density of people of the same age and sex as the patient. A negative Z-score of –2.5 or less should raise suspicion of a secondary cause of osteoporosis.

DETERMINATION AND ANALYSIS OF ARTHRITIS USING DIGITAL IMAGE PROCESSING TECHNIQUES

1BHAVYASHREE K G, 2SHEELA RAO N

1,2Department of Instrumentation Technology, Department of Instrumentation Technology, S.J.C.E., Mysore E-mail: bhavyagkshetty@gmail.com, sheelaraon@gmail.com

Arthritis is a common bone disease that mainly affects the joints of the body; basically fingers, hands, knees. This may lead to disability, premature mortality

and chronic ill-health. In this work, THERMAL images of knee have been used for analysis. The estimation of volume or thickness of cartilage at knee plays an important role in determining arthritis. The image is first preprocessed with B-Splines creation before segmentation. Then the edges are fine tuned with canny and log edge detectors. Finally the distance between the edges is calculated in order to find cartilage thickness.

Diagnosis of rheumatoid arthritis in knee using fuzzy C means segmentation technique

IEEE 24 November 2016 **Publisher:** IEEE
M Gobikrishnan ; T Rajalakshmi ; U Snekhalatha

Rheumatoid arthritis is a chronic inflammatory disease. It occurs mostly in joints such as wrist, bone and knee. Other than joints it also affects other parts in the body. Inflammation around the heart region and low red blood cell count are also possible causes of this disease. Although different imaging modalities like X-ray, THERMAL and CT are used to diagnose this disease. In recent days thermal imaging has proven to be more useful in medical imaging technique especially for disease diagnosing. Thermal imaging technique is based on infrared thermo grams, that shows a temperature variations in disease affected region. The main objective of this study is to diagnose the presence of rheumatoid arthritis using thermal imaging and to automatic segment the abnormal region in the knee.

Thermal image analysis and segmentation of hand in evaluation of rheumatoid arthritis

U. Snekhalatha ; M. Anburajan ; Therace Teena ; B. Venkatraman ; M. Menaka ; Baldev Raj

IEEE 01 March 2012

Rheumatoid arthritis (RA) is a chronic inflammatory disease that affects and destroys the joints of fingers, wrist and feet. Although different imaging modalities like x-ray, magnetic resonance imaging and ultrasound are available for diagnosing the RA. Thermal imaging is considered as a novel imaging technique for diagnosing the RA. Thermal imaging technique is based on infrared Thermograms depicting the temperature variations in abnormal region of interest. The objectives of this study was i) to evaluate the rheumatoid arthritis based on heat distribution index and skin temperature measurements and to analyse the difference in skin temperature measurement in hand for RA patients and normal persons. ii) to automatically segment the abnormal regions of the hand especially for arthritis patients using fuzzy c means algorithm and Expectation Maximization (EM) algorithm. In this work, thermal image analysis was done based on heat distribution index (HDI) and skin temperature measurement.

CHAPTER 2

THERMAL IMAGEING FOR BONE ANALYSIS

Digital Infrared Thermal Imaging (DITI) or Infrared Thermography is a non-invasive, non-contact, harmless technique which measures and records the surface temperature of the skin under study as thermogram or thermal images. Segmentation of the region of interest from thermal images is a very difficult task especially with the bone because of the presentation of the ankle bones in the images and the temperature difference between the bone and background being small which interfere with the segmentation task. Our segmentation procedure is

an attempt to work on these challenges and has shown promising results. In this work, a semi-automatic segmentation algorithm is proposed and implemented in MATLAB to segment the bone from thermal images taken using Fluke TiX560 thermal imaging camera. Image Acquisition protocol plays a very important role in successful segmentation of thermal images. Images acquired using different setups at three different occasions are considered for the current study.

Digital Infrared Thermal Imaging (DITI) [1], Digital Medical Thermal Imaging [2], [3] enables early diagnosis of certain medical conditions which goes unnoticed before causing pain, immobility or reduced quality of life. Human body has high emissivity of 0.98, close to that of black body and any rise in temperature due to inflammation or other medical condition can be easily captured in thermograms. This property of human body makes it feasible for modern thermal imagers to identify any medical condition causing the change in temperature before it can be identified by other traditional clinical assessment. Since each pixel of the thermal images (thermograms) acquired by the Infrared/Thermal Camera represents the energy radiated from the surface of the object under study as temperature readings, this technique has shown promising results in early diagnosis of some diseases like breast arthritis, diabetic neuropathy, osteoarthritis, rheumatoid arthritis, varicose veins and other blood circulation related conditions. Amputation is defined as severing or detachment of limbs by medical illness, trauma or surgery. Some of the major indications for performing amputations include malignancy, infection, gangrene and ischemia. The current rise in the incidence of vascular diseases secondary to diabetes and hypertension has resulted in a drastic increase in amputation procedures worldwide. Amputation, along with a cause of physical morbidity, carries with it significant emotional trauma. Patients who require amputations are prone to depression and a sense of failure. It is a momentous

decision that affects everyone involved, from the family of the patient to the surgeon. This demands an innovative technique for regular assessment of bone which is easy, safe and not uncomfortable for the patients and is cost-effective. Traditional assessment of the bone includes measurements of the subjective clinical variables, laboratory values and radiographic findings. There has been no automated analysis and detection from thermal images which will assist the specialized doctor in the early diagnosis and continuous assessment of the complication. The segmentation of the bone from the background in the thermal image is more complex because the bone is typically colder and the temperature difference between the bone and the background can be very small making segmentation through simple thresholding ineffective. Furthermore, infrared reflections on the backdrop cause the regions in the proximity of the bone to have similar intensity to the edges of the bone. Consequently, the bone cannot be segmented with a simple binarisation of the thermal image. Thermal images are hard to interpret and analyze manually by humans. For automation using the existing feature extraction and segmentation algorithms, it is difficult to find features that accurately segment the images. The main aim of this work is to automatically segment the bone from the thermal images which can be used later for analyzing any bone complication.

The segmented bone will be specifically useful in the early detection of bone complications in patients with Diabetes Mellitus and patients who are at high risk for these complications. The segmentation result will be used further in the following research objectives such as: (a) both the left and right feet may be restored to a general and unbiased bone contour template to reduce the asymmetry in the bone registration. (b) Combining the thermography technology with other modalities, such as photometric stereo imaging and multispectral imaging in the

experimental setup to predict the development or healing of diabetic bone complications. (d) Comparing the effectiveness and efficiency of predicting diabetic bone complications using different modalities. (e) Developing and investigating an intelligent telemedicine system with the most cost-effective modality or modalities to monitor diabetic bone status, thereby also adapting the usability and the operational conditions required in daily clinical practice as given. Thermograms in the frontal and lateral views of 23 individuals of both genders of the head and neck regions were taken with the FLIR SC655 camera, making a total of 46 thermal images [5]. The outcome of the study is a software that allows the user to select any ROI independently of its geometric shape. It also contains a segmentation algorithm based on Thresholding, which optimizes the chosen region by removing areas that don't have any relevant statistic data in order to take into account only the temperature of the ROI that will be used in further characterization. In [6], J. Gauci et al. carried out segmentation and extraction of specific points of interest from a set of thermal images of the shins, volar aspect of the hand and plantar aspect of the bone. They used these points as seeds to a region growing procedure that extracted areas on which the mean temperatures are computed. The work concludes that the procedure grows the area around the seed and never goes outside the body boundaries and the selected thresholds were thus found to be effective at detecting transitions from body to background. Visual image is segmented using a threshold set to the mean intensity of all pixels and the binary image of the segmented bone is used as a mask for segmenting the bone in the thermal image. The method proposed in [7] for segmentation and extraction of Region of Interest(ROI) in breast thermogram uses thresholding based on entropy followed by morphological processing. The thermal images are processed in two stages to segment the breast from the background using thresholding, texture analysis and morphological operations. In [4] segmentation was carried out by

rigidly registering the bone regions, detected in the color image to the thermal image. Shweta and Hemant in their work [8] have shown that the images processed using morphology operation is better than the original images and that will in turn be useful in problem diagnosis. Chanjuan Liu et.al in [9] have proposed a setup for acquiring thermal images of the bone in a controlled environment. They have used Active Contours without edges to automatically segment the bone from the background. They have shown that 7 out of 20 images required manual segmentation and also the ankle region was removed after segmentation using post-processing which is not discussed. Also the segmentation result was dependent on the initial position of the contours and noise in the images. The work done in [10] shows that Otsu thresholding method works well for thermal images. The review of thermography for early detection of diabetic neuropathy given in [11] shows the various methods used in acquiring and carrying out the experiments to identify the problem areas in bone. In [12], plantar angiosomes concept is used to identify different segments where possible ulcerations can happen to study the temperature variations in these regions. The work in [13] uses Otsu based thresholding and color based segmentation of the fuse cabinet for fault detection.

The optimal conditions and factors influencing the use of infrared thermography in humans as observed in [14] was taken as guidelines for setting up the experiment for acquiring the thermal images. Environmental Factors: Room Size: 20 feet x30 feet; Ambient Temperature: 22oC for evaluating extremities; Relative humidity: 50%; Source Radiation: All lights in the room were switched off so that the heat radiated from the lights does not influence the temperature readings. Care was taken so that no hot objects that contribute to the increase in temperature such as coffee were kept near the subjects to be imaged. All windows and doors were kept closed so that the temperature is stabilized inside the room and there is no variation

throughout the imaging process. Thermal Imager specifications: Fluke TiX560 camera with a spatial resolution of 320x240 pixels and capability for super resolution of 640x480 pixels. Thermal sensitivity is 0.05oC. Has autofocus capability and direct distance measurement from the imager to the imaging object.

B. Thermal Image Acquisition

The subjects were asked to sit for 15 minutes in the temperature controlled room so that the feet are relaxed and there is no influence of exercise or any other xhaustion due to movement. The camera was mounted on a tripod. The bone was then focused using the auto focus capability of the camera with the laser pointing to the bone so that the distance

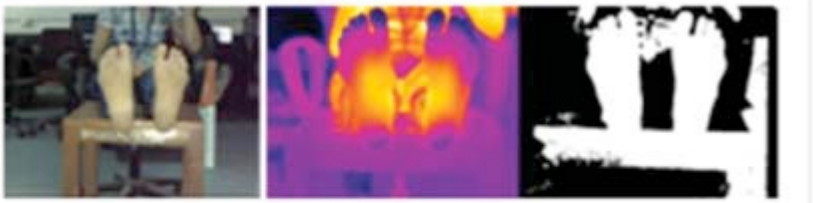

Fig.1. (a)Visual image (b)Thermal Image (C)Otsu Image

from the image to the camera is automatically obtained. A distance of 0.8 m was maintained approximately.

Imaging Setup -1:

The subjects were asked to sit on a chair and were asked to place their bone on a chair. Two images were taken for every subject. A total of 4 subjects were screened. Since the bone could not be segmented from the background, a

thermocol was used to hide the other parts of the body from appearing in the image. But segmenting in this setup was very difficult as it can be seen from the fig 2. Separating the bone from the leg part is a very challenging task as it has the same or slightly higher temperature than that of the bone.

Imaging Setup -1:

The subjects were asked to sit on a chair and were asked to place their bone on a chair. Two images were taken for every subject. A total of 4 subjects were screened. Since the bone could not be segmented from the background, a thermocol was used to hide the other parts of the body from appearing in the image. But segmenting in this setup was very difficult as it can be seen from the fig 2. Separating the bone from the leg part is a very challenging task as it has the same or slightly higher temperature than that of the bone.

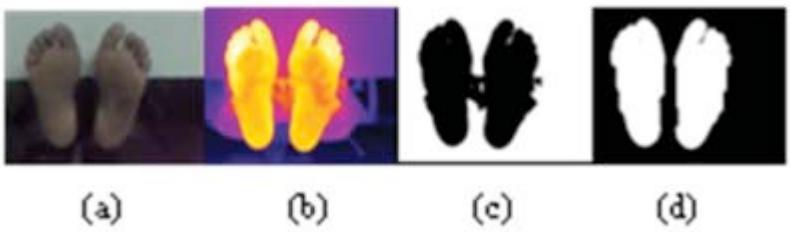

Fig. 2. (a)Visual Image (b)Thermal Image acquired using setup-1
(c)Segmented image by Otsu thresholding and (d)Segmented image using our method

Imaging Setup - 2:

Since segmentation was very difficult in setup-1, we came up with another setup where polyurethane foam [15] having density of 15Kg/m3 was used to hide the other parts of the body and to easily separate the bone from each other. Polyurethane foam was selected because of its good thermal insulation property

and easy availability (from local furniture and mattress shops used for cushioning). Two holes of size 10cm x 6 cm was made so that the bone can be inserted into each hole separately and the ankle portion could be prevented from appearing in the image. A total of 5 subjects were screened in this setup. But again, segmentation of the bone was not very impressive as the holes were little bigger and the foam was not stiff enough for good image. But there was a very good improvement in the segmentation result compared to the previous set up. It eliminates the effect of heat radiated by other parts of the body.

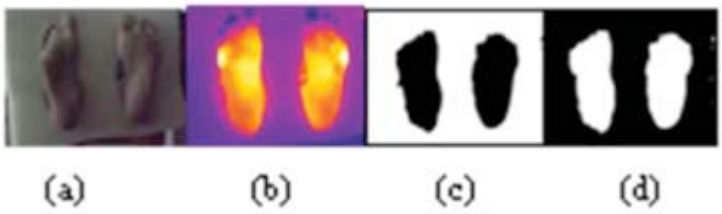

Fig. 3. (a)Visual Image (b)Thermal Image acquired using setup-2 (c)Segmented images by Otsu thresholding and (d)Segmented image using our method

Imaging Setup - 3:

The holes of the foam for inserting the bone in setup-2 are big as seen from the Fig.3. This includes the leg region also as part of the segmented bone which should be avoided. Hence another foam of density 30 Kg/m3 and two holes of size 8 cm x 5 cm was made so that the ankle is not seen as shown in Fig. 4. A total of 9 subjects were screened in this setup. There is comparable improvement in the mage with major part of the ankle covered.

Fig. 4 Imaging Setup-3

Fig 5. (a)Visual Image (b)Thermal Image acquired using setup-3 (c)Segmented image by Otsu thresholding and (d)Segmented image using our method

Manual Segmentation

The thermal images are segmented using the Image Segmenter application. Image Segmenter is an application in Image Processing and Computer Vision toolbox which can be found under the APPS tab of Matlab R 2013b. The ground truth segmentation is obtained using the freehand tool of the Image Segmenter. This gives the manually segmented image of the bone which is the ground truth in our case.

ii. Automatic Segmentation

a. The thermal images are first segmented using Ostu thresholding method.

b. The region involving the ankle is cropped

interactively using image processing toolbox in MATLAB. This ensures that the other parts of the bone remain the same and only the ankle region which poses challenge in segmentation is processed.

c. Morphological operation of closing which is dilation followed by erosion of the image is done on the cropped region. Morphological operations differ in how they carry out this comparison. The basic idea here is to probe an image with a small shape or template known as a structuring element to quantify the way the structuring element fits within a given image.

1. First, a disk structuring element of radius 40 pixels is used to probe the cropped region performing morphological closing of the region. Then, a rectangle structuring element of size 120x20 pixels is used to perform the closing operation on the previously closed image region.

2. The morphologically closed region is then overlaid automatically on the original image in the same location of the cropped region so that the effect is seen in the original image keeping the toes and other regions intact.

3. The segmented binary image is stored for comparison.

4. The segmented image after morphological processing is overlaid on top of the Otsu thresholded image to see the difference.

The segmented image obtained following our approach and the manually segmented image are compared side by side visually and through various other measures explained in the following section. It clearly shows that our approach

eliminates the problem of ankle bone in thermal images and both the images look alike as it can be observed from Fig. 7.

(a) (b)

Fig. 7. (a)Manually Segmented Image (b)Segmented image using our Method

D. Need for accurate segmentation

The success or failure of detection of any anomaly in a particular subject of study is often a direct consequence of the success or failure of segmentation. Also, if the edge detections are accurate then the thresholds too are as mentioned in [16]. To make sure that while retrieving the bone images of a particular patient from the database at a later date for assessing the complication, it might be possible that the images of two different persons might match if not accurately segmented. Accurate segmentation of the bone will ensure accurate registration of the bone to avoid these problems. Temperature difference for any diagnosis is kept as 2oC which might be contributed by inaccurate segmentation results (in this case the ankle region) which leads to false detection of a bone complication.

CHAPTER 3

IMAGE RESTORATION

The simplest and best investigated diffusion method for smoothing images is to apply a linear diffusion process. We shall focus on the relation between linear diffusion filtering and the convolution with a Gaussian, analyze its smoothing properties for the image as well as its derivatives, and review the fundamental properties of the Gaussian scale-space induced by linear diffusion filtering.

(a). Anisotropic Diffusion

Perona and Malik propose a nonlinear diffusion method for avoiding the blurring and localization problems of linear diffusion filtering. They apply an inhomogeneous process that reduces the diffusivity at those locations which have a

larger likelihood to be edges. This likelihood is measured by $|\nabla u|^2$. The Perona–Malik filter is based on the equation

$$\partial_t u = \mathrm{div}\,(g(|\nabla u^2)\,\nabla u) \qquad (3.1)$$

and it uses diffusivities such as

$$g(s^2) = 1/(1 + (s^2/\lambda^2))\ (\lambda > 0) \qquad (3.2)$$

Although Perona and Malik name their filter anisotropic, it should be noted that – in our terminology – it would be regarded as an isotropic model, since it utilizes a scalar-valued diffusivity and not a diffusion tensor. In 1984 Cohen and Grossberg proposed a model of the primary visual cortex with similar inhibition effects as in the Perona–Malik model. The experiments of Perona and Malik were visually very impressive: edges remained stable over a very long time. It was demonstrated that edge detection based on this process clearly outperforms the linear Canny edge detector, even without applying non-maxima suppression and hysteresis thresholding. This is due to the fact that diffusion and edge detection interact in one single process instead of being treated as two independent processes which are to be applied subsequently. Moreover, there is another reason for the impressive behaviour at edges, which we shall discuss next

It is a well-known fact that images usually contain structures at a large variety of scales. In those cases where it is not clear in advance which is the right scale for the depicted information it is desirable to have an image representation at multiple scales. Moreover, by comparing the structures at different scales, one obtains a hierarchy of image structures which eases a subsequent image interpretation. A scale-space is an image representation at a continuum of scales, embedding the image f into a family $\{Ttf|t| \geq 0\}$ of gradually simplified versions of it, provided that it fulfils certain requirements. Most of these properties can be

classified as architectural, smoothing (information-reducing) or invariance requirements. An important architectural assumption is recursive, i.e. for t 0, the scale space representation gives the original image f, and the filtering may be split into a sequence of filter banks:

$$T_0 f = f \qquad (3.3.2.3)$$

$$T_{t+s} f = T_t(T_s f) \; \forall s, t \geq 0 \qquad (3.3.2.4)$$

This property is very often referred to as the semigroup property. Other architectural principles comprise for instance regularity properties of Tt and local behavior as t tends to 0.

Smoothing properties and information reduction arise from the wish that the transformation should not create artifacts when passing from fine to coarse representation. Thus, at a coarse scale, it should not have additional structure swhich are caused by the filtering method itself and not by underlying structures at finer scales. This simplification property is specified by numerous authors in different ways, using concepts such as no creation of new level curves (causality), non-enhancement of local extrema decreasing number of local extrema , maximum loss of figure impression, Tikhonov regularization, maximum–minimum principle, positivity preservation of positivity, comparison principle, and Lyapunov functionals. Especially in the linear setting, many of these properties are equivalent or closely related.

It may regard an image as a representative of an equivalence class containing all images that depict the same object. Two images of this class differ e.g. by grey level shifts, translations and rotations or even more complicated transformations such as affine mappings. This makes the requirement plausible that

the scale-space analysis should be invariant to as many of these transformations as possible, in order to analyse only the depicted object.

The pioneering work of Alvarez, Guichard, Lions and Morel shows that every scale-space fulfilling some fairly natural architectural, information-reducing and invariance axioms is governed by a PDE with the original image as initial condition. Thus, PDEs are the suitable framework for scale-spaces. Often these requirements are supplemented with an additional assumption which is equivalent to the superposition principle, namely linearity:

$$T_t(af+ bg) = a\ T_t f+ b\ T_t g \forall t \geq 0, \quad \forall a, b \in IR \qquad (3.3)$$

As we shall see below, imposing linearity restricts the scale-space idea to essentially one representative.

There is a simple way of modifying the linear scale space paradigm to achieve the objectives that it has put forth in the previous section. In the diffusion equation frame work of looking at scale-space, the diffusion coefficient c is assumed to be a constant independent of the space location. There is no fundamental reason why this must be so. To quote Koenderink “I do not permit space variant blurring. Clearly this is not essential to the issue, but it simplifies the analysis greatly.” It will show how a suitable choice of $c\ (\ x\ ,\ y,\ t\ )$ will enable to satisfy the second and third criteria listed in the previous section. Furthermore this can be done without sacrificing the causality criterion.

Consider the anisotropic diffusion equation

$$\boldsymbol{I}, = \ div\ (\ c\ (\ x\ , y, t\ )\ \nabla l\ )\ \ =\ \ \boldsymbol{c}(\boldsymbol{x}, y.r)\Delta l\ +\ \nabla c\ \nabla I \qquad (3.4)$$

Where it is indicate with *div* the divergence operator, and with ∇ and Δrespectively the gradient and Laplacian operators, with respect to the space variables. It reduces

to the isotropic heat diffusion equation $\boldsymbol{I_t = c\,\Delta I}$ if $c(x, y, t)$ is a constant. Suppose that at the time (scale) t, it is known the locations of the region boundaries appropriate for that scale. It would want to encourage smoothing *within* a region in preference to smoothing *across* the boundaries. This could be achieved by setting the conduction coefficient to be 1 in the interior of each region and 0 at the boundaries. The blurring would then take place separately in each region with no interaction between regions. The region boundaries would remain sharp.

Of course it is *not* known in advance the region boundaries at each scale (if it is done the problem would already have been solved!). What can be computed is a current best estimate of the location of the boundaries (edges) appropriate to that scale.

Let $\boldsymbol{E(x, y, t)}$ be such an estimate: a vector-valued function defined on the image which ideally should have the following properties:

1) $\boldsymbol{E(x, y, t) = 0}$ in the interior of each region.
2) $\boldsymbol{E(x, y, t) = Ke(x, y, t)}$ at each edge point,

where $\boldsymbol{e}$ is a unit vector normal to the edge at the point, and $\boldsymbol{K}$ is the local contrast (difference in the image intensities on the left and right) of the edge.

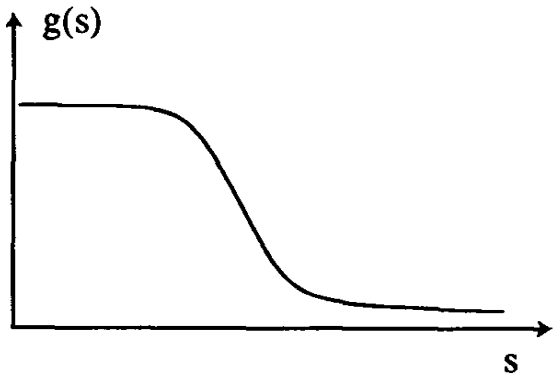

Fig. 3.2 The qualitative shape of the nonlinearity g (.)

Note that the word ***edge*** as used above has not been formally defined-it means here the perceptual subjective notion of an edge as a region boundary. A completely satisfactory formal definition is likely to be part of the solution, rather than the problem definition!

If an estimate $\boldsymbol{E}(\boldsymbol{x}, y, \boldsymbol{t})$ is available, the conduction coefficient $\boldsymbol{c}(\boldsymbol{x}, y, t)$ can be chosen to be a function $\boldsymbol{c} = g(\|\boldsymbol{E}\|)$ of the magnitude of $\boldsymbol{E}$. According to the previously stated strategy $g(.)$ has to be a nonnegative monotonically decreasing function with $g(0) = 1$. This way the diffusion process will mainly take place in the interior of regions, and it will not affect the region boundaries where the magnitude of $\boldsymbol{E}$ is large.

It is intuitive that the success of the diffusion process in satisfying the three scale-space goals of will greatly depend on how accurate the estimate $\boldsymbol{E}$ is as a "guess" of the position of the edges. Accuracy though is computationally expensive and requires complicated algorithms. It is able to show that fortunately the simplest estimate of the edge positions, the gradient of the brightness function, i.e., $\boldsymbol{E}(\boldsymbol{x}, y, \boldsymbol{t}) = \nabla \boldsymbol{I}(\mathbf{x}, y, t)$, gives excellent results.

There are many possible choices for $g(\ )$, the most obvious being a binary valued function. It would show that in case the edge estimate :

$\boldsymbol{E}(\boldsymbol{x}, y, \boldsymbol{t}) = \nabla \boldsymbol{I}(\mathbf{x}, y, t)$ the choice of $g(\ )$ is restricted to a subclass of the monotonically decreasing functions.

(b). Properties of Anisotropic diffusion filter

Anisotropic diffusion satisfies the causality criterion by recalling a general result of the partial differential equation theory, the maximum principle. It

is shown that a diffusion in which the conduction coefficient is chosen locally as a function of the magnitude of the gradient of the brightness function, i.e.,

$$c(x, y, t)=g(||\nabla \boldsymbol{I}(x, y, t)||) \quad (3.5)$$

will not only preserve, but also sharpen, the brightness edges if the function *g* (.) is chosen properly.

A discrete form of the anisotropic diffusion filter described in was proposed by Perona and Malik as follows:

$$u_{i,j}^{n+1} = u_{i,j}^{n} + {}^{\lambda}/_{4} \cdot [c_N \cdot \nabla_N u + c_S \cdot \nabla_S u + c_E \cdot \nabla_E u + c_W \cdot \nabla_W u]_{i,j}^{n} \quad (3.6)$$

where $\lambda \in [0,1]$ controls the rate of diffusion. Usually a small value λ is used to avoid destabilizing the diffusion process. The letters N, S, E and W (north, south, east, and west) describethe direction of the local gradient. The local gradient is calculated using nearest-neighbor differences

$$\begin{aligned} \nabla_N u_{i,j} &= u_{i-1,j} - u_{i,j} \\ \nabla_S u_{i,j} &= u_{i+1,j} - u_{i,j} \\ \nabla_E u_{i,j} &= u_{i,j+1} - u_{i,j} \\ \nabla_W u_{i,j} &= u_{i,j-1} - u_{i,j} \end{aligned} \quad (3.7)$$

Different functions were used for *g* (-) giving perceptually similar results. The images in this project were obtained using

$$g(\nabla I)=\frac{1}{1+\left(\frac{||\nabla I||}{K}\right)^2} \quad (3.8)$$

where K is a constant that is tuned for a particular application.

3.3.2 IMAGE ENHANCEMENT

(a). Adaptive Mean Adjustment

This is a computer image processing technique used to improve contrast in images. It differs from ordinary histogram equalization in the respect that the adaptive method computes several histograms, each corresponding to a distinct section of the image, and uses them to redistribute the lightness values of the image. It is therefore suitable for improving the local contrast of an image and bringing out more detail.

However, AHE has a tendency to over-amplify noise in relatively homogeneous regions of an image. A variant of adaptive histogram equalization called **contrast limited adaptive histogram equalization** (CLAHE) prevents this by limiting the amplification.

(b). Contrast Enhancement

There is a strong influence of contrast ratio on resolving power and detection capability of images. Techniques for improving image contrast are among the most widely used enhancement processes. The sensitivity range of any remote sensing detector is designed to record a wide range of terrain brightness from black basalt plateaus to White Sea beds under a wide range of lighting conditions. Few individual scenes have a brightness range that utilizes the full sensitivity range of these detectors. To produce an image with the optimum contrast ratio, it is important to utilize the entire brightness range of the display medium, which is generally film.

The purpose of image restoration is to "compensate for" or "undo" defects which degrade an image. Degradation comes in many forms such as motion blur, noise, and camera misfocus. In cases like motion blur, it is possible to come up with a very good estimate of the actual blurring function and "undo" the blur to restore the

original image. In cases where the image is corrupted by noise, the best we may hope to do is to compensate for the degradation it caused. In this project, we will introduce and implement several of the methods used in the image processing world to restore images.

(c). Degradation Model

The block diagram for our general degradation model is

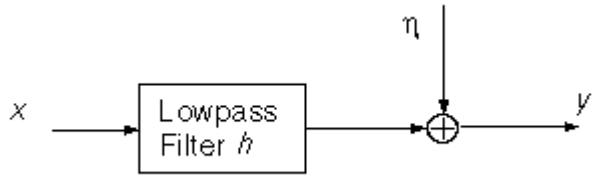

Fig 3.3 Degradation Model

where g is the corrputed image obtained by passing the original image f through a low pass filter (blurring fuction) b and adding noise to it.

Fig 3.4 Noised Image

To understand what adaptive median filtering is all about, one first needs to understand what a median filter is and what it does. In many different kinds of digital image processing, the basic operation is as follows: at each pixel in a digital

image we place a neighborhood around that point, analyze the values of all the pixels in the neighborhood according to some algorithm, and then replace the original pixel's value with one based on the analysis performed on the pixels in the neighborhood. The neighborhood then moves successively over every pixel in the image, repeating the process.

The algorithm is applied to each pixel of the noisy image in order to identify whether it is uncorrupted or corrupted. After such an application to the entire image, a two-dimensional binary decision map is formed at the end of the noise detection stage, with 0s indicating the positions of uncorrupted pixels, and 1s for those corrupted ones.

The boundary discriminative process consists of two iterations, in which the second iteration will only be invoked conditionally. In the first iteration, an enlarged local window with a size of 21x21 (empirically determined) is used to examine whether the considered pixel is an uncorrupted one.

Noise is any undesired information that contaminates an image. Impulse noise is a special type of noise, which have many different origins. The Salt and Pepper type impulse noise is typically caused by malfunctioning of the pixel elements in the camera sensors, faulty memory locations, or timing errors in the digitization process. For the images corrupted by Salt and Pepper noise, the noisy pixels can take only the maximum or the minimum values in the dynamic range.

1. Less effective in removing Gaussian or random-intensity noise. The median filter can remove noise only if the noisy pixels occupy less than one half of the neighborhood area.

2. Repeating will remove noise but at the expense of detail (posterization occurs) where pixel brightness values are leveled across regions "group of pixels having similar brightness values
3. High computational cost (for sorting N pixels, the temporal complexity is O(N·logN), When the median filter must be carried out in real time, the software implementation in general-purpose processors does not usually give good results and FPGAs are a good alternative
4. Some median algorithms are not good for real time processing.
5. The median filter gives brightness differences resulting in maximal blurring of regional boundaries.
6. Median computer algorithm cannot be customized.

(d). Impulse Detection

In an image contaminated by random-valued impulse noise, the detection of noisy pixel is more difficult in comparison with fixed valued impulse noise, as the gray value of noisy pixel may not be substantially larger or smaller than those of its neighbours. Due to this reason, the conventional median-based impulse detection methods do not perform well in case of random valued impulse noise. In order to overcome this problem, we use a non linear function to transform the pixel values within the filter window W(x) (i, j) in a progressive manner. This operation widens the gap between noisy pixel x (i,j) and the other pixels in the window W(x) (i, j). In the beginning of each iteration, the central pixel x (i,j) of each window is subtracted from all the pixels in the window and normalized absolute differences are obtained

D(m,n)= |X(m,n)- x(i,j) |/255; x(m,n)

$$d(m,n) = \left| x(m,n) - x(i,j) \right| / 255; x(m,n) \in W^{(x)}(i,j) \cdots\cdots 2$$

The normalized absolute differences, are then transformed by a nonlinear function to increase the gap between the differences d(m, n) corresponding to noisy pixels and those due to noise-free Pixels

$$d^{(t)}(m,n) = e^{K.d(m,n)} - 1;$$

$$m = i - L, \ldots, i + L, n = j - L, \ldots, j + L$$

where d(t)(m, n) denotes the transformed value of d(m, n)and K is a constant which varies with iterations. The transformed values d(t)(m, n) are sorted as {d(t)(1)≤ d(t)(2)≤…. ≤ d(t)(9)}in ascending order where { d(t)(1), d(t)(2), ….., d(t)(9)} are the transformed values{d(m, n)} of . Now, the central pixel is considered noisy for a filtering window of size 3X3 if . The output of the detector is represented by a binary flag image {f(I, j)}, where f(i, j) = 1 indicates that the pixel x(i, j) is noisy; for noiseless pixel, f(i, j) = 0.

3.3.4 SEGMENTATION

Image segmentation was, is and will be a major research topic for many image processing researchers. The reasons are obvious and applications endless: most computer vision and image analysis problems require a segmentation stage in order to detect objects or divide the image into regions which can be considered homogeneous according to a given criterion, such as color, motion, texture, etc.

Clustering is the search for distinct groups in the feature space. It is expected that these groups have different structures and that can be clearly differentiated. The clustering task separates the data into number of partitions, which are volumes in the n-dimensional feature space. These partitions define a hard limit between the different groups and depend on the functions used to model the data distribution.

Image segmentation is the first step in image analysis and pattern recognition. It is a critical and essential component of image analysis system, is one of the most difficult tasks in image processing, and determines the quality of the final result of analysis. Image segmentation is the process of dividing an image into different regions such that each region is homogeneous.

Image segmentation methods can be categorized as follows (this is not an exhaustive list):

1. **Histogram thresholding:** assumes that images are composed of regions with different gray (or colour) ranges, and separates it into a number of peaks, each corresponding to one region.
2. **Edge-based approaches:** use edge detection operators such as Sobel, Laplacian for example. Resulting regions may not be connected, hence edges need to be joined.
3. **Region-based approaches:** based on similarity of regional image data. Some of the more widely used approaches in this category are: Thresholding, Clustering, Region growing, Splitting and merging.
4. **Hybrid:** consider both edges and regions.

The project is done using Image Segmentation by Clustering. It is based on Color image segmentation using Mahalanobis distance. Euclidean distance is also used for comparing between the quality of segmentation between the Mahalanobis and Euclidean distance.

3.3.4.1 Image Segmentation by Clustering

Clustering is a classification technique. Given a vector of N measurements describing each pixel or group of pixels (i.e., region) in an image, a similarity of

the measurement vectors and therefore their clustering in the N-dimensional measurement space implies similarity of the corresponding pixels or pixel groups. Therefore, clustering in measurement space may be an indicator of similarity of image regions, and may be used for segmentation purposes.

The vector of measurements describes some useful image feature and thus is also known as a feature vector. Similarity between image regions or pixels implies clustering (small separation distances) in the feature space. Clustering methods were some of the earliest data segmentation techniques to be developed.

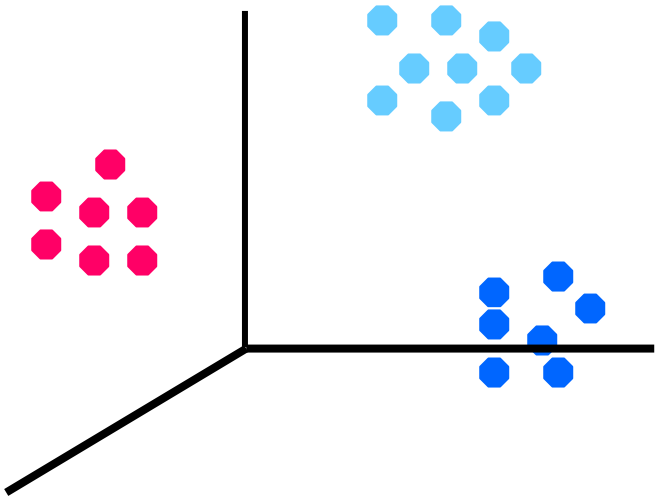

Fig 3.3.4.1 Similar data points grouped together into clusters.

Most popular clustering algorithms suffer from two major drawbacks

First, the number of clusters is predefined, which makes them inadequate for batch processing of huge image databases.

Secondly, the clusters are represented by their centroid and built using an Euclidean distance therefore inducing generally an hyperspheric cluster shape, which makes them unable to capture the real structure of the data. This is especially true in the case of color clustering where clusters are arbitrarily shaped

3.3.4.2 Clustering Algorithms:

- **K-means**
- **FCM**

There are many other algorithms used for clustering.

3.3.4.2.1 K-Means Clustering Overview

K-Means clustering generates a specific number of disjoint, flat (non-hierarchical) clusters. It is well suited to generating globular clusters. The K-Means method is numerical, unsupervised, non-deterministic and iterative.

3.3.4.2.2 Clustering properties

- There are always K clusters.
- There is always at least one item in each cluster.
- The clusters are non-hierarchical and they do not overlap.
- Every member of a cluster is closer to its cluster than any other cluster because closeness does not always involve the center of clusters.

3.3.4.2.3 The K-Means Algorithm Process

1. The dataset is partitioned into K clusters and the data points are randomly assigned to the clusters resulting in clusters that have roughly the same number of data points.
2. For each data point:
3. Calculate the distance (Mahalanobis or Euclidean) from the data point to each cluster.
4. If the data point is closest to its own cluster, leave it where it is. If the data point is not closest to its own cluster, move it into the closest cluster.
5. Repeat the above step until a complete pass through all the data points results in no data point moving from one cluster to another. At this point the clusters are stable and the clustering process ends.
6. The choice of initial partition can greatly affect the final clusters that result, in terms of inter-cluster and intra-cluster distances and cohesion.

Flow-chart of an image segmentation method

Step 1:

First, an image is taken as an input. The input image is in the form of pixels and is transformed into a feature space (RBG).

Step 2:

Next similar data points, i.e. the points which have similar color, are grouped together using any clustering method. A clustering method such as k-means clustering is used to form clusters as shown in the flow chart. The distances are calculated using Mahalanobis and Euclidean distant.

The above figure shows how the data points are clustered in the 3-d RGB space. As one can see all similar colors are grouped together to form a cluster.

The data points with minimum Mahalanobis distance or Euclidean distance are grouped together to form the clusters. Mahalanobis and Euclidean are described later below.

Step 3:

After clustering is done, the mean of the clusters is taken. Then the mean color in each cluster is calculated to be remapped onto the image.

3.3.4.2.4 Cluster analysis

Clustering is the classification of objects into different groups, or more precisely, the partitioning of a data set into subsets (clusters), so that the data in each subset (ideally) share some common trait - often proximity according to some defined distance measure. Data clustering is a common technique for statistical data analysis, which is used in many fields, including machine learning, data mining, pattern recognition, image analysis and bioinformatics. The computational task of classifying the data set into k clusters is often referred to as **k-clustering**.

Besides the term data clustering (or just clustering), there are a number of terms with similar meanings, including cluster analysis, automatic classification, numerical taxonomy, botryology and typological analysis.

Both of the algorithms under consideration date back originally over 30 years. A K-Means algorithm was introduced by name in 1967 while an EM algorithm was somewhat formalized ten years later in 1977. The dates attached to these algorithms can be somewhat confusing since the EM algorithm can be considered a generalized K-Means algorithm. It is safe to assume that both algorithms existed previously without formalization or a complete explanation of the theory involved. In order to understand how to implement each algorithm, the class notes and

Wikipedia were relied on heavily. In addition, a few of the papers found in the references section were of limited assistance.

The K-Means algorithm and the EM algorithm can both be used to find natural clusters within given data based upon varying input parameters. Clusters can be formed for images based on pixel intensity, color, texture, location, or some combination of these. For both algorithms the starting locations of the partitions used are very important and can make the difference between an optimal and a non-optimal solution since both are susceptible to termination when achieving a local maximum as opposed to the global maximum.

K-Means can be thought of as an algorithm relying on hard assignment of information to a given set of partitions. At every pass of the algorithm, each data value is assigned to the nearest partition based upon some similarity parameter such as Euclidean distance of intensity. The partitions are then recalculated based on these hard assignments. With each successive pass, a data value can switch partitions, thus altering the values of the partitions at every pass. K-Means algorithms typically converge to a solution very quickly as opposed to other clustering algorithms.

3.3.4.2.5 Methodology

Two K-Means algorithms have been implemented. The first clusters the pixel information from an input image based on the RGB color of each pixel, and the second clusters based on pixel intensity. The algorithm begins with the creation of initial partitions for the data. The clustering based on pixel color will be considered first.

In order to try to improve the runtime and results of the algorithm, partitions which are equally spaced were chosen. Initially, eight partitions were chosen. The

partitions represented red, green, blue, white, black, yellow, magenta, and cyan or the corners of the "color cube". With the initial partitions chosen, the algorithm can begin. Every pixel in the input image is compared against the initial partitions and the nearest partition is chosen and recorded. Then, the mean in terms of RGB color of all pixels within a given partition is determined. This mean is then used as the new value for the given partition. If a partition has no pixels associated with it, it remains unchanged. In some implementations, a partition with no pixels associated with it would be removed; however, these partitions are simply ignored in this implementation. Once the new partition values have been determined, the algorithm returns to assigning each pixel to the nearest partition. The algorithm continues until pixels are no longer changing which partition they are associated with or, as is the case here, until none of the partition values changes by more than a set small amount. In order to gather more results, the initial partitions used were varied by adding and removing partitions.

In a nearly identical setup, a second K-Means implementation was made using the grayscale intensity of each pixel rather than the RGB color to partition the image. The starting partitions were chosen as equally spaced values from 0 to 255. The number of partitions used, as in the color segmenting setup, was varied in order to increase the number of results available and to study the effects of varying this parameter.

For this case, the same initial partitions as used in the color segmentation with K-Means were used in order to make the comparison of results more meaningful. Here, RGB color was again chosen as the comparison parameter.

$$E[z_{ij}] = \frac{p(x = x_i \mid \mu = \mu_j)}{\sum_{n=1}^{k} p(x = x_i \mid \mu = \mu_n)}$$

$$= \frac{e^{-\frac{1}{2\sigma^2}(x_i-\mu_j)^2}}{\sum_{n=1}^{k} e^{-\frac{1}{2\sigma^2}(x_i-\mu_n)^2}}$$

This equation states that the expectations or weight for pixel z with respect to partition j equals the probability that x is pixel x_i given that μ is partition μ_i divided by the sum over all partitions k of the same previously described probability. This leads to the lower expression for the weights. The sigma squared seen in the second expression represents the covariance of the pixel data. Once the E step has been performed and every pixel has a weight or expectation for each partition, the M step or maximization step begins. This step is defined by the following equation:

$$\mu_j \leftarrow \frac{1}{m} \sum_{i=1}^{m} E[z_{ij}]\, x_i$$

This equation states that the partition value j is changed to the weighted average of the pixel values where the weights are the weights from the E step for this particular partition. This EM cycle is repeated for each new set of partitions until, as in the K-Means algorithm, the partition values no longer change by a significant amount.

The following images demonstrate the k-means clustering algorithm in action, for the two-dimensional case. The initial centres are generated randomly to demonstrate the stages in more detail.

3.3.4.2.6 Applications of the algorithm

The k-means clustering algorithm is commonly used in computer vision as a form of image segmentation. The results of the segmentation are used to aid border detection and object recognition. In this context, the standard euclidean distance is usually insufficient in forming the clusters. Instead, a weighted distance measure utilizing pixel coordinates, RGB pixel color and/or intensity, and image texture is commonly used.

3.3.4.2.7 Model of fuzzy c-mean method (FCM)

The standard FCM is an iterative, unsupervised clustering algorithm, initially developed by FCM algorithm introduced. The following model of FCM is described.

The Observed THERMAL signal is modeled as a product of the true signal generated by the underlying anatomy, and a spatially varying factor called the gain field

$$Y_k = X_k G_k \qquad \forall k \in \{1, 2, \cdots, N\} \qquad (1)$$

groups the values X_k, Y_k and G_k are the true intensity, observed intensity and the gain field at the kth voxel, respectively. N is the total number of pixels in the THERMAL volume.

The application of a logarithmic transformation to the intensities allows the artifact to be modeled as an additive bias field

$$y_k = x_k + \beta_k \qquad \forall k \in \{1, 2, \cdots, N\} \qquad (2)$$

where x_k and y_k are the true and observed log-transformed intensities at the kth voxel, respectively, and β_k is the bias field at the kth voxel. If the gain field is known, then it is relatively easy to estimate the tissue class by applying a

conventional intensity-based segmentation to the corrected data. The following discussion is based the model of (2) and estimation of the gain field β_k.

CHAPTER 4

Adaptive Mean Shift Fuzzy C Means Segmentation or Modified FCM algorithm (M-FCM)

In the followings, we will introduce some modifications to this algorithm. The evaluation of the method for localized measurements, such as the impact on tumour boundary or volume determinations also needs further work.

$$J_m = \sum_{i=1}^{c} \sum_{k=1}^{N} u_{ik}^{p} \| y_k - \beta_k - v_i \|^2 + \sum_{i=1}^{c} \sum_{k=1}^{N} u_{ik}^{p} \Big(\sum_{y_r \in N_k} w(y_k, y_r) \| y_r - \beta_r - v_i \|^2 \Big) \qquad (3)$$

Where $w(y_k, y_r)$ is a weighting function, satisfied the following conditions

$$\sum_{y_r \in N_k} w(y_k, y_r) = \alpha,\ 0 \le \alpha < 1,\ \forall k \in \{1, 2, \cdots, N\}$$

especially, when $w(y_k, y_r) = \dfrac{\alpha}{N_R}$, the J_m is MFCM objective function(3) proposed.

Formally, the optimization problem is estimated those parameters in the form

$$\min_{u_{i,k}, v_i, \beta_k} J_m \tag{4}$$

The objective function can be calculated as the MFCM algorithm. Taking the first derivatives of J_m with respect to u_{ik}, v_i, β_k, and setting them to zero results in three necessary but not sufficient conditions for J_m to be at a local maximum. In the following sections, we derive these estimating results and propose the algorithm..

A. Membership Evaluation

$$u_{ik}^* = \frac{1}{\sum_{j=1}^{c} \left(\frac{D_{ik} + \gamma_{ik}}{D_{ij} + \gamma_{ij}} \right)^{1/(p-1)}} \tag{5}$$

where $D_{ik} = \| y_k - \beta_k - v_i \|^2$, and $\gamma_{ik} = \sum_{y_r \in N_k} w(y_k, y_r) \| y_r - \beta_r - v_i \|^2$

B. Cluster Prototype Updating

$$v_i^* = \frac{\sum_{k=1}^{N} u_{ki}^p \left((y_k - \beta_k) + \sum_{y_r \in N_k} w(y_k, y_r)(y_r - \beta_r) \right)}{\sum_{k=1}^{N} u_{ki}^p (1 + \sum_{y_r \in N_k} w(y_k, y_r))} \tag{6}$$

C. Bias-Field Estimation

$$\beta_k^* = y_k - \frac{\sum_{i=1}^{c} v_i \left(u_{ik}^p + \sum_{y_r \in N_k} w(y_k, y_r) u_{ir}^p \right)}{\sum_{i=1}^{c} \left(u_{ik}^p + \sum_{y_r \in N_k} w(y_k, y_r) u_{ir}^p \right)} \tag{7}$$

D. The discuss of the convergence

Theory: if $w(y_k, y_r) \geq 0$ and

$\sum_{y_r \in N_k} w(y_k, y_r) = \alpha,\ 0 \leq \alpha < 1,\ \forall k \in \{1, 2, \cdots, N\}$ and N_k is a 4 or 8 – connective neighborhood.

Then objective function J_m is convergence.

M-FCM Algorithm

The M-FCM algorithm for correcting the bias field and segmenting the image into different clusters can be summarized in the following steps.

Step 1: Select the Weighting function, in general,

$$w(y_k - y_r) = \alpha e^{-\frac{\|y_k - y_r\|^2}{\sigma^2}} \qquad (8)$$

where $0 \le \alpha < 1, \sigma \ge 1$;

Step 2: Select initial class prototypes $\{v_i\}_{i=1}^{c}$, for example

$$\left\{ v_i = \log(255 * (2i-1)/2c) \right\}_{i=1}^{c}$$

Set $\{\beta_k\}_{k=1}^{N}$ to equal and very small values (e.g., 0.01).

Step 3: Update the partition matrix using (5)

Step 4: The prototypes of the clusters are obtained in the form of weighted averages of the patterns using (6).

Step 5: Estimate the bias term using (7).

Repeat Steps 3)–5) till termination. The termination criterion is as follows:

$$\|V_{new} - V_{old}\| < \varepsilon \qquad (9)$$

where $\|\cdot\|$ is the Euclidean norm, V is a vector of cluster centres, and ε is a small number that can be set by the user (e.g., 0.01).

We describe the application of the M-FCM segmentation on synthetic images corrupted with multiplicative gain and real T1 bone thermal images. Simulating image is a T1-weighted phantom with in-plane high resolution, Gaussian noise

with 6.0, and three-dimensional linear shading 7% in each direction. There are many advantages for using digital phantoms rather than real image including in prior knowledge of the true tissue types and control over image parameters such as mean intensity values, noise and intensity in homogeneities. We also employed the fast algorithm improving calculation effect, because its consumed time is 1/4 of the

Fig 3.3.4.2.9 Various types of clustering procedures

Clustering is the process of grouping feature vectors into classes in the self-organizing mode. Let $\{\mathbf{x}^{(q)}: q = 1,\ldots,Q\}$ be a set of Q feature vectors. Each feature vector $\mathbf{x}^{(q)} = (x_1^{(q)}, \ldots, x_N^{(q)})$ has N components. The process of clustering is to assign the Q feature vectors into K clusters $\{\mathbf{c}^{(k)}: k = 1, \ldots, K\}$ usually by the minimum distance assignment principle.

Choosing the representation of cluster centers (or prototypes) is crucial to the clustering. Feature vectors that are farther away from the cluster center should not have as much weight as those that are close. These more distant feature vectors are

outliers usually caused by errors in one or more measurements or a deviation in the processes that formed the object.

The simplest weighting method is arithmetic averaging. It adds all feature vectors in a cluster and takes the average as prototype. Because of its simplicity, it is still widely used in the clustering initialization.

The arithmetic averaging gives the central located feature vectors the same weights as outliers. To lower the influence of the outliers, median vectors are used in some proposed algorithms.

To be more immune to outliers and more representative, the fuzzy weighted average is introduced to represent prototypes:

$$\mathbf{Z}_n^{(k)} = \sum_{\{q:\, q \in k\}} w_{qk} \mathbf{x}^{(q)}_n; \qquad (10)$$

Rather than a Boolean value 1 (true, which means it belongs to the cluster) or 0 (false, does not belong), the weight w_{qk} in equation (10) represent partial membership to a cluster. It is called a fuzzy weight. There are different means to generate fuzzy weights.

One way of generating fuzzy weights is the reciprocal of distance

$$w_{qk} = 1/ D_{qk}, \ (w_{qk} = 1 \text{ if } D_{qk} = 0) \qquad (11)$$

It was used in earlier fuzzy clustering algorithms. When the distance between the feature vector and the prototype is large, the weight is small. On the other hand, it is large when the distance is small.

Using Gaussian functions to generate fuzzy weights is the most natural way for clustering. It is not only immune to outliers but also provides appropriate weighting for more centrally and densely located vectors. It is used in the fuzzy clustering and fuzzy merging (FCFM) algorithm.

In this project, we implemented the fuzzy c-means (FCM) algorithm and the fuzzy clustering and merging algorithm in Java, applied the algorithms to several data sets and compared the weights of the two algorithms.

The segmentation of imaging data involves partitioning the image space into different cluster regions with similar intensity image values. The most medical images always present overlapping gray-scale intensities for different tissues. Therefore, Modified fuzzy clustering methods are particularly suitable for the segmentation of medical images. There are several Modified FCM clustering applications in the THERMAL segmentation of the bone. The Modified Fuzzy c-means (FCM) can be seen as the fuzzified version of the k-means algorithm. It is a method of clustering which allows one piece of data to belong to two or more clusters. This method is frequently used in pattern recognition. The algorithm is an iterative clustering method that produces an optimal c partition by minimizing the weighted within group sum of squared error objective function.

CHAPTER 5

PATIENT TRACKING

Health related issues and parameters are of utmost importance to man, and is essential to his existence and influence and thus he has sought for an improved system that would be able to capture and monitor the changes in health parameters

irrespective of time and location so as to provide for measures that will forestall abnormalities and cater for emergencies. This work presents a pacemaker fault analysis that is capable of providing real time remote monitoring of the heartbeat with improvements of an alarm and SMS alert. This project aims at the design and implementation of a low cost but efficient and flexible heartbeat monitoring and alert system using GSM technology. It is designed in such a way that the heartbeat/pulse rate is sensed and measured by the sensors which sends the signals to the control unit for proper processing and determination of the heartbeat rate which is displayed on an LCD, it then proceeds to alert by an alarm and SMS sent to the mobile phone of the medical expert or health personnel, if and only if the threshold value of the heartbeat rate is maximally exceeded. Thus this system proposes a continuous, real time, remote, safe and accurate monitoring of the heartbeat rate and helps in patient‟s diagnosis and early and preventive treatment of cardiovascular ailments.

Cardiovascular disease is one of the main causes of death in many countries and thus it accounts for the over 15 million deaths worldwide. In addition, several million people are disabled by cardiovascular disease [1]. The delay between the first symptom of any cardiac ailment and the call for medical assistance has a large variation among different patients and can have fatal consequences. One critical inference drawn from epidemiological data is that deployment of resources for early detection and treatment of heart disease has a higher potential of reducing fatality associated with cardiac disease than improved care after hospitalization. Hence new strategies are needed in order to reduce time before treatment. Monitoring of patients is one possible solution. Also, the trend towards an independent lifestyle has also increased the demand for personalized non-hospital based care. Cardiovascular disease has shown that heart beat rate plays a key role

in the risk of heart attack. Heart disease such as heart attack, coronary heart disease, congestive heart failure, and congenital heart disease is the leading cause of death for men and women in many countries. Most of the time, heart disease problems harm the elderly person. Very frequently, they live with their own and no one is willing to monitor them for 24 hours a day [1].

In this proposed device, the heart beat and temperature of patients are measured by using sensors as analog data, later it is converted into digital data using analog to digital converter (ADC) which is suitable for wireless transmission using SMS messages through GSM modem. Micro controller device is used for temporary storage of the data used for transmission [2]. For a patient who is already diagnosed with fatal heart disease, their heart rate condition has to be monitored continuously. This project proposes and focuses on the design of the heartbeat monitor that is able to monitor the heart beat rate condition of patient continuously. This signal is processed using the microcontroller to determine the heart beat rate per minute. Then, it sends short message service (SMS) alert to the mobile phone of medical experts or patient‟s family members, or their relatives about the condition of the patient and abnormal details via SMS. Thus, doctors can monitor and diagnose the patient‟s condition continuously and could suggest earlier precaution for the patients themselves. This will also alert the family members to quickly attend to the patient. The remote heartbeat monitor proposed in this work can be used in hospitals and also for patients who can be under continuous monitoring while traveling from place to place,since the system is continuously monitoring the patient.

BACKGROUND STUDY

Recent breakthroughs in science and technological innovations have led to an unprecedented advancement in provisions of technological solutions for the numerous problems facing mankind. Researchers are busy leveraging on modern technology to provide better and improved solutions commensurate to the ever increasing demands. A heart rate monitor is a personal monitoring device that allows one to measure one's heart rate in real time or record the heart rate for later study. Early models consisted of a monitoring box with a set of electrode leads which attached to the chest. The first wireless electrocardiogram (ECG) heart rate monitor was invented in 1977 as a training aid for the Finnish National Cross Country Ski team and as 'intensity training' became a popular concept in athletic circles in the mid-80s, retail sales of wireless personal heart monitors started from 1983 [3]. In old versions of the monitor, when a heartbeat is detected a radio signal is transmitted, which the receiver uses to determine the current heart rate. This signal can be a simple radio pulse or a unique coded signal from the chest strap (such as Bluetooth or other low-power radio link); the latter prevents one user's receiver from using signals from other nearby transmitters (known as cross-talk interference) [3]. Newer versions of the heart rate monitor include a microprocessor which is continuously monitoring the ECG and calculating the heart rate, and other parameters. Modern heart rate monitors usually comprise two elements: a chest strap transmitter and a wrist receiver or mobile phone (which usually doubles as a watch or phone). In early plastic straps, water or liquid was required to get good performance. Later units have used conductive smart fabric with built-in microprocessors which analyses the ECG signal to determine heart rate. More advanced models will offer measurements of heart rate variability, activity, and breathing rate to assess parameters relating to a subject's fitness. Sensor fusion algorithms allow these monitors to detect core temperature and dehydration [3]. The digital heartbeat monitor and alert systems provides a more

unique, effective and efficient means of real-time monitoring of a patient‟s health parameters and has ever since witnessed an unprecedented tremendous advancement as researchers keep searching for better ways to make these monitoring and alert systems more flexible, portable, and efficient. This section presents a review of current research findings and works done so far by different researchers with the same mindset of providing flexible, portable, and efficient monitoring and alert systems.

FUNCTIONAL UNITS OF THE SYSTEM

A Power Supply Unit

This unit was developed around, built and incorporated in the board. The power supply source for the system would be mains AC. The circuit would use a 12v DC and consists of the rectifier diode, smoothening capacitor and the voltage regulator.

GSM Shield/Module

The GSM Shield allows a board to connect to the internet, make/receive voice calls and send/receive SMS messages. The shield uses a radio modem M10 by Quectel (datasheet). It is possible to communicate with the board using AT commands. The GSM library has a large number of methods for communication with the shield. The shield uses digital pins 2 and 3 for software serial communication with the M10. The M10 is a Quad-band GSM/GPRS modem that works at frequencies GSM850MHz, GSM900MHz, DCS1800MHz and PCS1900MHz. It supports TCP/UDP and HTTP protocols through a GPRS connection. As always with board, every element of the platform – hardware, software and documentation is freely available and open-source. A GSM module assembles a GSM modem with

standard communication interfaces like RS-232 (Serial Port), USB etc., so that it can be easily interfaced with a computer or a microprocessor / microcontroller based system. The power supply circuit is also built into the module and can be activated using a suitable adaptor. Like a GSM mobile phone, a GSM modem requires a SIM card from a wireless carrier in order to operate. The GSM/GPRS module is designed to enable communication between the microcontroller and GMS network. The GSM/GPRS MODEM can perform the following operations:

1. Receive, send or delete SMS messages in a SIM.
2. Read, add, search phonebook entries of the SIM.
3. Make, Receive, or reject a voice call.

It is recommended that the board be powered with an external power supply that can provide between 700mA and 1000mA. Powering an PIC and the GSM shield from a USB connection is not recommended, as USB cannot provide the required current for when the modem is in heavy use. The modem can pull up to 2A of current at peak usage, which can occur during data transmission.

The Pulse Sensor Unit

A Heartbeat sensor is a monitoring device that allows one to measure his or her heart rate in real time or record the heart rate for later study. It provides a simple way to study the heart function. This sensor monitors the flow of blood through the finger and is designed to give digital output of the heartbeat when a finger is placed on it. When the sensor is working, the beat LED flashes in unison with each heartbeat. This digital output can be connected to the microcontroller directly to measure the Beats per Minute (BPM) rate. It works on the principle of light modulation by blood flow through finger at each pulse [7]. The Pulse Sensor is a

well-designed plugand play heart-rate sensor for PIC. It also includes an open-source monitoring app that graphs your pulse in real time. The Pulse Sensor can be connected to PIC with jumpers. The Code for Hardware and Software otherwise known asThe Processing code is called „P_PulseSensor_xx“ ,running this code on this data visualization software gives: The group of three numbers on the left correspond to the pulse waveform peak, trough, and amplitude. At the top of the screen, a smaller data window graphs heart rate over time. This graph advances every pulse, and the Beats Per Minute is updated every 10 heart pulses. The big red heart also pulses to the time of your heartbeat. When you hold the Pulse Sensor to your fingertip, you should see a nice saw-tooth waveform like the one above. The pulse sensor amped is a greatly improved version of the original pulse sensor. This version incorporates amplification and noise cancellation circuitry into the hardware, making it much more reliable. It is compatible with 3.3 and 5v microcontrollers giving you more flexibility and the processing visualization software and PIC code have been streamlined and improved.PIC watches the analog signal from pulse sensor, and a pulse is found when the signal rises above the mid-point, that's the moment when the capillary tissue gets slammed with a surge of fresh blood. When the signal drops below the mid-point, PIC sees this and gets ready to find the next pulse. The digital pulses are given to the microcontroller for calculating the heat beat rate, given by the formula- BPM (Beats per minute) = 60*fWhere f is the pulse frequency. We have built in hysteresis to the rising and falling thresholds which can be adjusted if necessary [8].

LCD Display Unit

Liquid Crystal Display (LCD) modules that display characters such as text and numbers are the most cheapest and simplest to use of all LCDs. They can be

purchased in various Sizes, which are measured by the number of rows and columns of characters they can display. Any LCD with an HD44780- or KS0066-compatible interface is compatible with PIC. A 16x2 LCD display is very basic electronic module and is very commonly used in various devices and circuits. These modules are preferred over seven segments and other multi segment LEDs because they are economical, easily programmable, has no limitation of displaying special and even custom characters (unlike in seven segments), animations and so on . A **16x2 LCD** means it can display 16 characters per line and there are 2 such lines. In this LCD each character is displayed in 5x7 pixel matrix. This LCD has two registers, namely, Command and Data. The command register stores the command instructions given to the LCD. A command is an instruction given to LCD to do a predefined task like initializing it, clearing its screen, setting the cursor position, controlling display etc. The data register stores the data to be displayed on the LCD. The data is the ASCII value of the character to be displayed on the LCD.

Buzzer

A **buzzer** or beeper is an audio signaling device, which may be mechanical, electromechanical, or piezoelectric and finds extensive use in electronics circuits and designs especially to trigger an alarm or as a system alert device. The buzzer is simply powered with a regulated 5v.

Mobile User

The mobile user is simply any GSM mobile phone that is able to send and receive an SMS. The microcontroller issues control signal which instructs the GSM

Module to send an SMS remotely over the GSM network to the GSM Mobile phone which receives the message sent to it. The GSM Module and the program algorithm can also be designed that the SMS message sent is to multiple predefined mobile users.

SYSTEM EVALUATION

This system is programmed such that it will sense and monitor the heartbeat rate whenever a fingertip is placed on the pulse sensor and triggers an alert by SMS messages sent to the mobile of the health personnel and also buzz an alarm whenever the critical threshold value of the heartbeat rate is exceeded. The table below shows the summary of the entire system performance as well as the tests carried out on the entire system to ascertain if it‟s working according to the desired objectives and specifications intended for it. The entire system is evaluated based on the tests, observations and results captured in the table below.

System Testing

This stage involves the testing of the whole system. After the integration of the whole units a test program was written and burnt into the microcontroller and then the system monitored to ensure optimum performance. The heart rate reading was displayed on the LCD in BPM.

Packaging

Several factors led to the type of packaging adopted, which includes mechanical damage protection, moisture protection, portability, cost, convenience, etc. The packaging was carried out using a plastic material called Perspex or acrylic glass. The finished product is shown below:

RESULTS

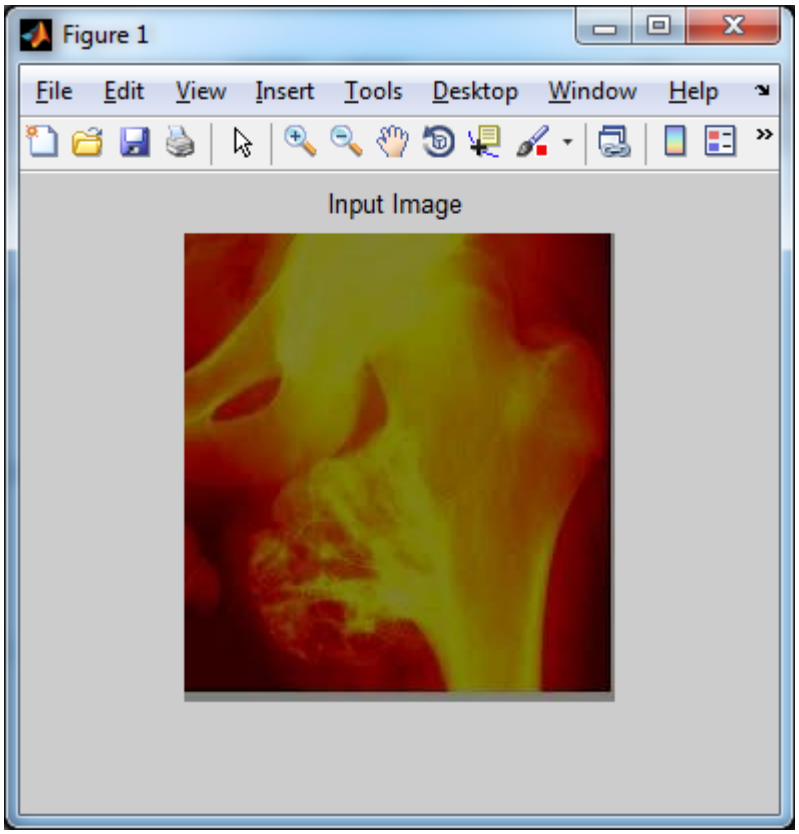
Figure 1
File Edit View Insert Tools Desktop Window Help
Input Image

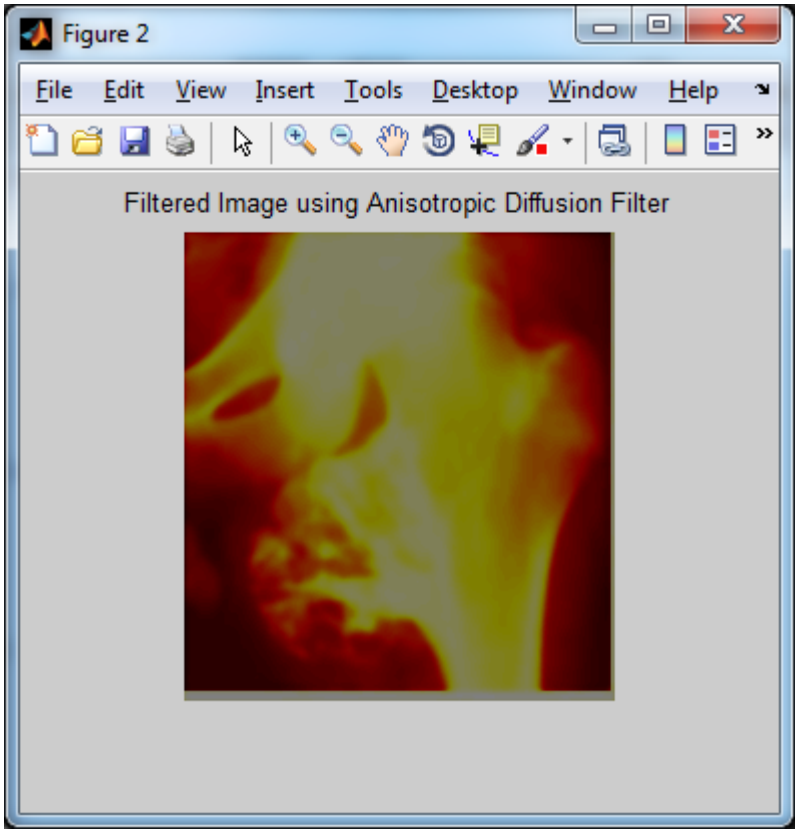
Figure 2
File Edit View Insert Tools Desktop Window Help
Filtered Image using Anisotropic Diffusion Filter

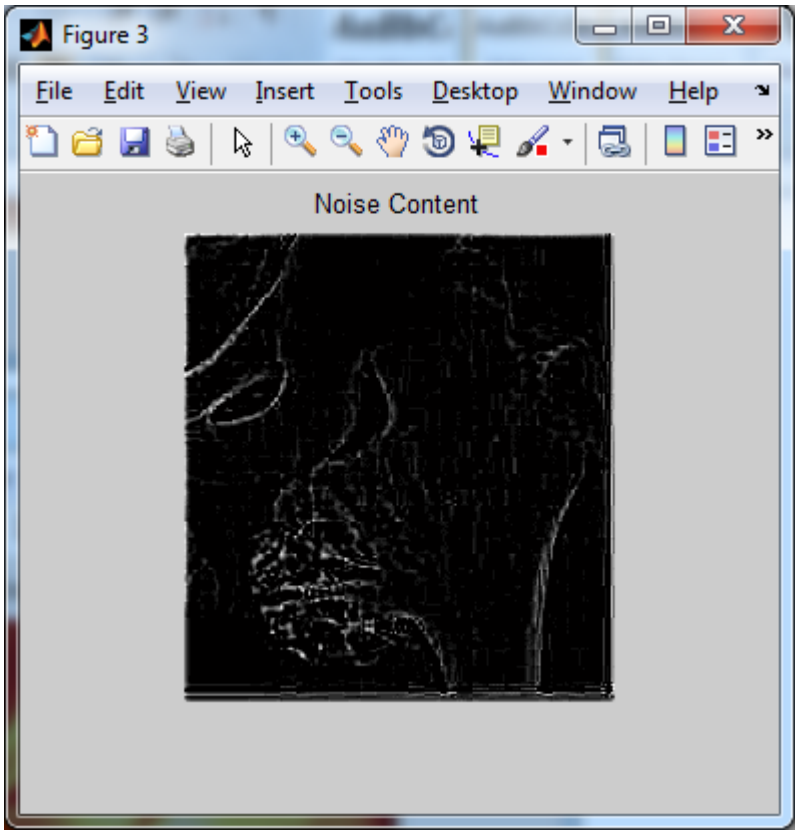
Figure 3
File Edit View Insert Tools Desktop Window Help
Noise Content

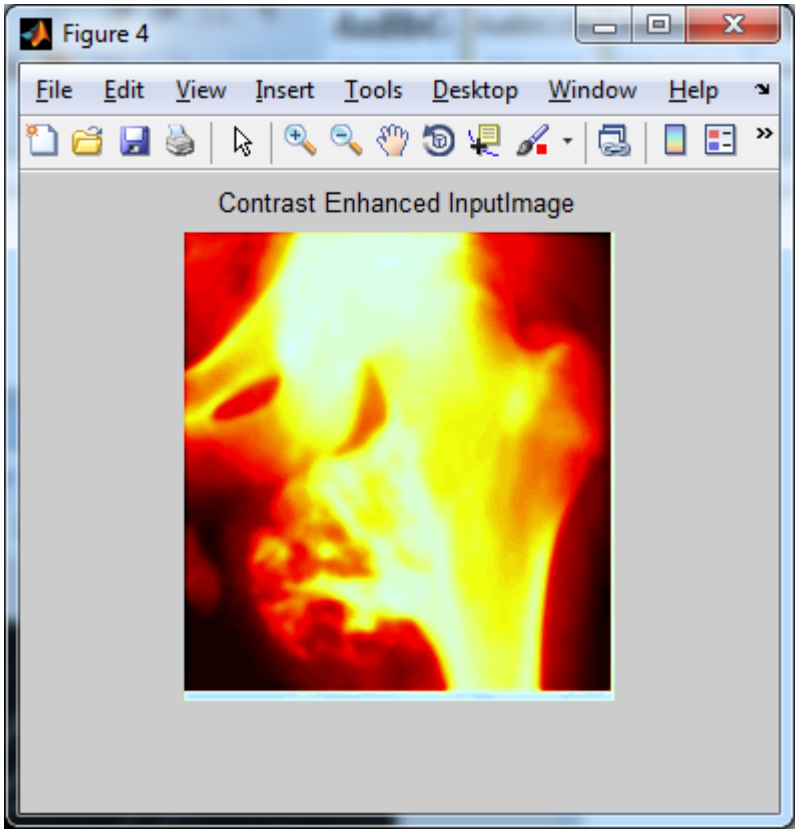
Figure 4
File Edit View Insert Tools Desktop Window Help
Contrast Enhanced InputImage

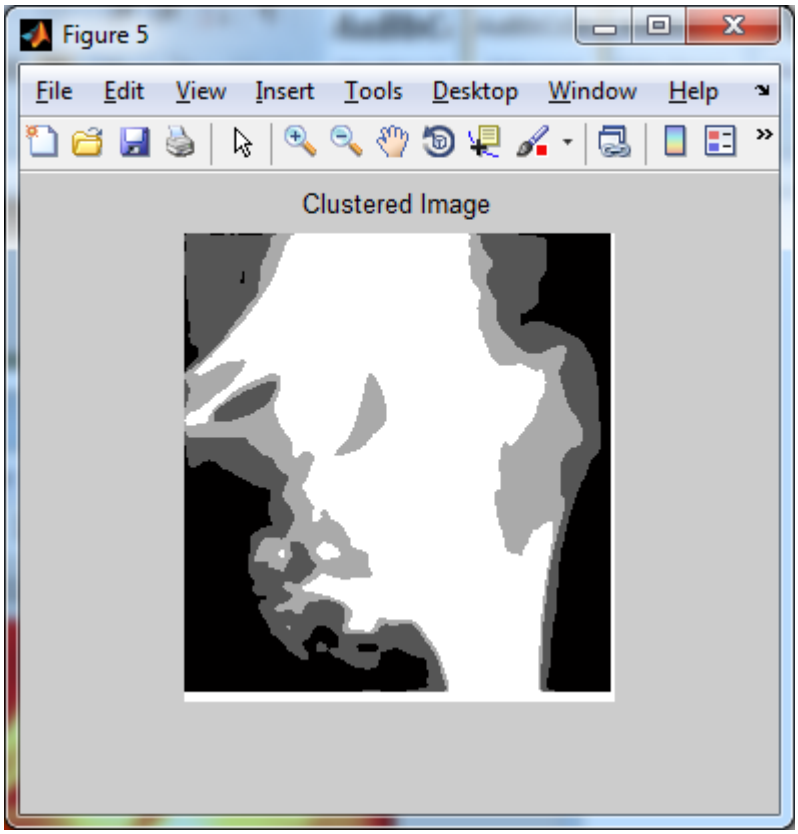
Figure 5
File Edit View Insert Tools Desktop Window Help
Clustered Image

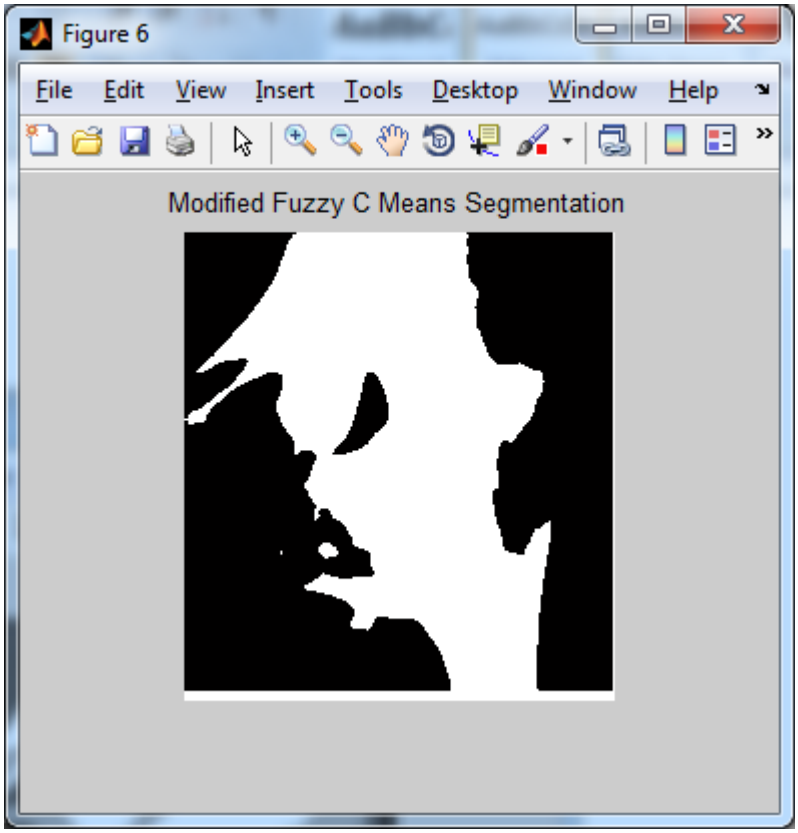
Figure 6
File Edit View Insert Tools Desktop Window Help
Modified Fuzzy C Means Segmentation

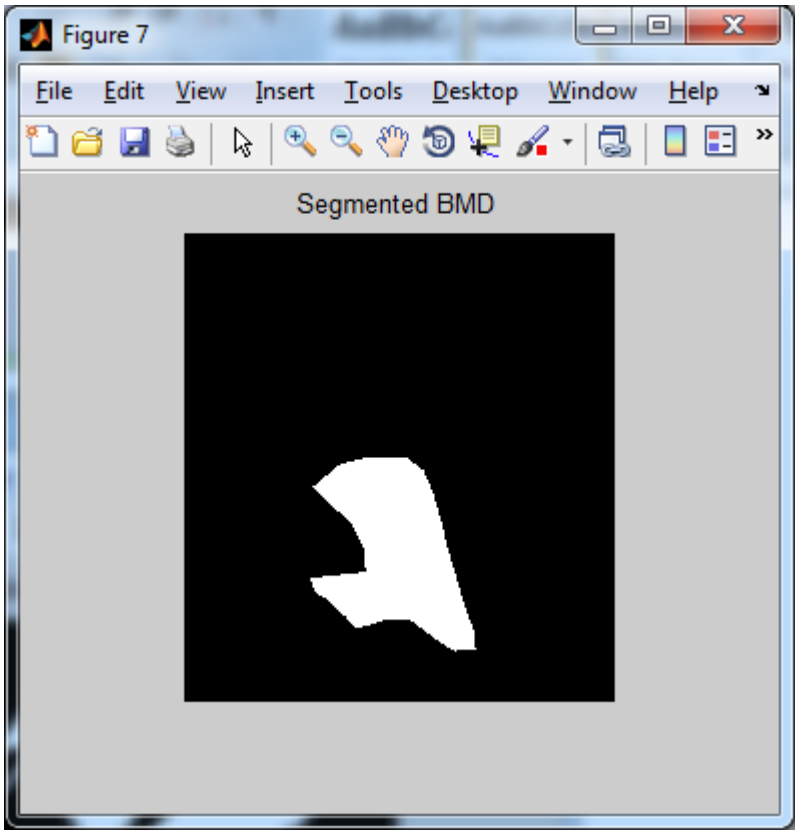
Figure 7
File Edit View Insert Tools Desktop Window Help
Segmented BMD

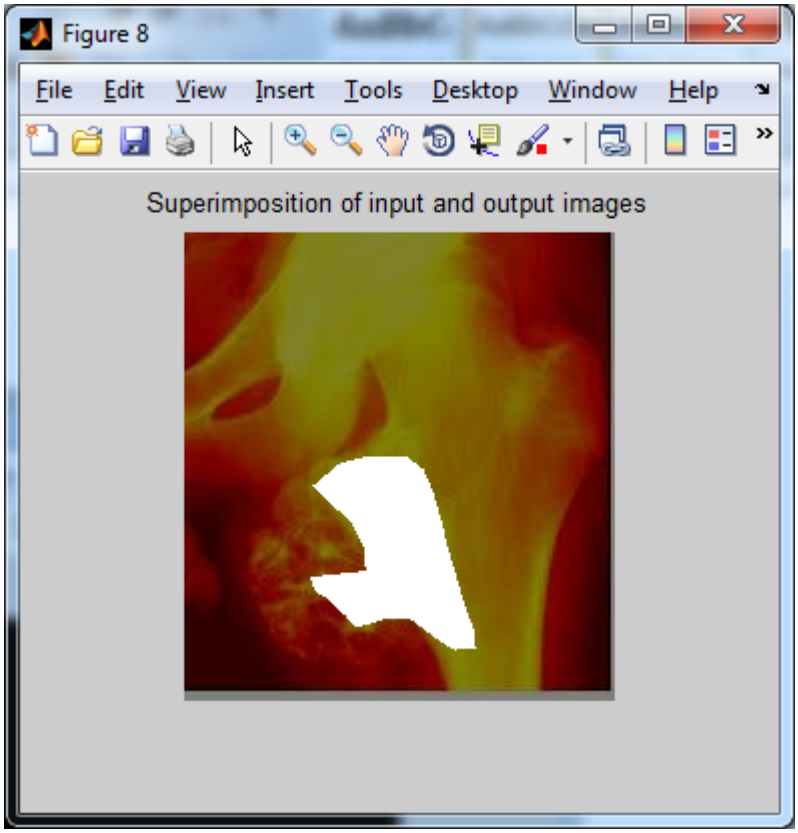
Figure 8
File Edit View Insert Tools Desktop Window Help
Superimposition of input and output images

CONCLUSION

The visualization of quantitative result helps in determining and analysis of the arthritis disease. The method is simple and efficient in attaining the aim of early arthritis detection based on cartilage thickness. This algorithm can be improved further by implementing automated technique for threshold selection. The results presented here are preliminary and focused only the reproducibility aspects of the technique. This technique is being applied towards monitoring early stage rheumatoid arthritis patients in an ongoing clinical trial. Results obtained from the clinical trial data should provide a better understanding. The present article provides thought of better understanding towards the disease in comparative way.

FUTURE WORK

Imaging techniques continue to significantly impact clinical diagnostics and basic science research including drug discovery. However, fluorescence and nanotechnology paralleled with imaging science facilitating precise localization with contrast visualization. Fluorescence imaging and nanocarriers are the most pertinent techniques that have been widely applied in research, diagnostics, and disease prognosis. Moreover, photoacoustics and ultrasound imaging have been gaining significant attention. In this chapter we have discussed recent innovation in fluorescence techniques, nanocarriers with imagining techniques for disease diagnosis and prognosis, and sensitive imaging techniques applied in molecular biology and clinics.

References

[1] Lau E, Symmons D, Bankhead C, MacGregor A, Donnan S, Silman A. Low prevalence of rheumatoid arthritis in the urbanized Chinese of Hong Kong. J Rheumatol 1993; 20: 1133-1137.

[2] Sugimoto H, Takeda A, Hyodoh K. Early-stage rheumatoid arthritis: prospective study of the effectiveness of R imaging for diagnosis. Radiology 2000; 216:569- 575.

[3] Gilkeson G, Polisson R, Sinclair H, et al. Early detection of carpal erosions in patients with rheumatoid arthritis: pilot study of magnetic resonance imaging. J Rheumatol 1988; 15: 1361-1366.

[4] Gasson J, Gandy SJ, Hutton CW, Jacoby RK, Summers IR, Vennart W. Magnetic resonance imaging of rheumatoid arthritis in metacarpophalangeal joints. Skeletal Radiol 2000; 29:324-334.

[5] Rau R, Herbon G. Healing phenomena of erosive changes in rheumatoid arthritis patients undergoing disease-modifying antirheumatic drug therapy Arthritis Rheum 1996; 39:162-168.

[6] Iannuzzi L, Dawson N, Zein N, Kushner I. Does drug therapy slow radiographic deterioration in rheumatoid arthritis? N Engl J Med 1983; 309:1023-1028.

[7] P.P. Cheung, M. Dougados, L. Gossec. “Reliability of ultrasonography to detect synovitis in rheumatoid arthritis: asystematic literature review of 35 studies (1,415 patients)” Arthritic Care Res (Hoboken). 2010 Mar; 62(3):323-34.Review. PMID: 20391478 [PubMedindexed for Medline]

[8] J.E. Freeston, P. Bird, P.G. Conaghan. “The role of MRI in rheumatoid arthritis research and clinical issues.”

Curr Opin Rheumatol. 2009 Mar; 21(2):95-101. Review. PMID: 19339918 [PubMed-indexed for Medline].

[9] F. McQueen, M. Ostergaard, C. Peterfy, M. Lassere, B. Ejbjerg, P. Bird, P. O'Connor, H. Genant, R. Shnier,
P.Emery, J. Edmonds, P. Conaghan, “Pitfalls in scoring MR images of rheumatoid arthritis wrist and metacarpophalangeal joints”. Ann Rheum Dis. 2005 February; 64(Suppl 1): i48–i55. doi: 10.1136/ard.2004.031831.
[10] M.A. Cimmino, M. Parodi, E. Silvestri et al. “Correlation between radiographic, echographic and MRI changes and rheumatoid arthritis progression.” Reumatismo, 2004 Jan-Mar; 56(1 Suppl 1): 28-40. Italian. PMID: 15201938 [PubMed-indexed for Medline]
[11] M. Aubry-Frize, G.R.C. Quartey, H. Evans, D. LaPalme, “The Thermographic Detection of Pain”. Proc. 3rd Canadian Clinical Engineering Conf., pp. 82-83, Saskatoon, SK, 1981.
[12] Collins, A.J., Ring, E.F.J., Cosh, J.A. and Bacon, P.A. “Quantification of Thermography in Arthritis Using Multi Isothermal Analysis”, Annals of the Rheumatic Diseases, Vol. 33, pp. 113-115, 1974.
[13] M.D. Devereaux, G.R. Parr, D.P. Page Thomas, B.L. Hazleman, “Disease Activity Indexes in Rheumatoid
Arthritis; a Prospective, Comparative Study with Thermography”, Annals of Rheumatic Diseases, Vol. 44, pp. 434-437, 1985.
[14] www.mathwork.com [15]THRASOS N. PAPPAS ‘New Challenges for Image Processing Research’ IEEE TRANSACTIONS ON IMAGE PROCESSING, VOL. 20, NO. 12, DECEMBER 2011
[16] The Physics of Medical Imaging Book by Steve Webb published by CRC Press Taylor &Francis group 2012